Inorganic Chemistry

Article

pubs.acs.org/IC

Mononuclear Five- and Six-Coordinate Iron Hydrazido and Hydrazine Species

Caroline T. Saouma, Connie C. Lu,† and Jonas C. Peters*

Division of Chemistry and Chemical Engineering, California Institute of Technology, Pasadena, California 91125, United States

Supporting Information

ABSTRACT: This article describes the synthesis and characterization of several low-spin iron(II) complexes that coordinate hydrazine (N_2H_4), hydrazido ($N_2H_3^-$), and ammonia. The sterically encumbered tris(di-*meta*-terphenylphosphino)borate ligand, $[PhBP^{mter}_3]^-$, is introduced to provide access to species that cannot be stabilized with the $[PhBP^{Ph}_3]^-$ ligand ($[PhBP^{R}_3]^-$ = $PhB(CH_2PR_2)_3^-$). Treatment of $[PhBP^{mter}_3]FeMe$ with hydrazine generates the unusual 5-coordinate hydrazido complex $[PhBP^{mter}_3]Fe(\eta^2\text{-}N_2H_3)$ (**1**), in which the hydrazido serves as an L_2X-type ligand. Upon coordination of an L-type ligand, the hydrazido shifts to an LX-type ligand, generating $[PhBP^{mter}_3]Fe(L)(\eta^2\text{-}N_2H_3)$ (L = N_2H_4 (**2**) or NH_3 (**3**)). In contrast, treatment of $[PhBP^{Ph}_3]FeMe$ with hydrazine forms the adduct $[PhBP^{Ph}_3]Fe(Me)(\eta^2\text{-}N_2H_4)$ (**5**). Complex **5** is thermally unstable to methane loss, generating intermediate $[PhBP^{Ph}_3]Fe(\eta^2\text{-}N_2H_3)$, which undergoes bimolecular coupling to produce $\{[PhBP^{Ph}_3]Fe\}_2(\mu\text{-}\eta^1\text{:}\eta^1\text{-}N_2H_4)(\mu\text{-}\eta^2\text{:}\eta^2\text{-}N_2H_2)$. The oxidation of these and related hydrazine and hydrazido species is also presented. For example, oxidation of **1** or **5** with $Pb(OAc)_4$ results in disproportionation of the N_2H_x ligand (x = 3, 4), and formation of $[PhBP^{R}_3]Fe(NH_3)(OAc)$ (R = Ph (**9**) and *m*ter (**11**)).

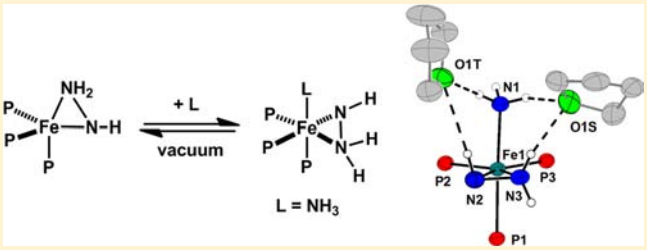

INTRODUCTION

An area of ongoing research is geared toward elucidating the mechanism by which N_2 is reduced to NH_3 at the FeMo-cofactor of nitrogenase.[1] Recent spectroscopic studies of the enzyme acquired under turnover conditions suggest that N_2 initially coordinates an iron center.[2] Though the mechanism of subsequent N_2 reduction remains unknown, the ability of the cofactor to reduce both diazene and hydrazine implicates that an alternating reduction scheme may be viable.[3] In this mechanistic scenario, the delivery of protons and electrons alternates between the two nitrogen atoms (i.e., N≡N → HN═NH → H_2N–NH_2 → $2NH_3$). To explore the chemical feasibility of such a mechanistic scheme, model complexes that coordinate N_2H_x ligands are warranted.

In addition to their proposed role in N_2 reduction, hydrazine (N_2R_4), hydrazido ($N_2R_3^-$), and hydrazido(2−) ($N_2R_2^{2-}$) species have also been invoked as reactive intermediates in several synthetic transformations, including the hydrohydrazination and diamination of alkynes.[4] In light of this, most studies on $M(N_2R_3)$ species feature substituted hydrazido ligands,[5] and a comparatively small subset feature the parent hydrazido ($N_2H_3^-$) functionality.[6] This relative scarcity may also be due in part to the different inherent stabilities of $M(N_2R_x)$ and $M(N_2H_x)$ species.[6l,7]

Terminal hydrazido species of the type $M(\eta^1\text{-}N_2H_3)$ were first prepared in the 1970s by both Chatt[6a] and Hidai[6b] (M = W). Since then, examples of Mo,[6k] Re,[6c] Fe,[6d,n] and Ru[6n] $M(\eta^1\text{-}N_2H_3)$ complexes have been characterized. Side-on hydrazido species, $M(\eta^2\text{-}N_2H_3)$, are also uncommon; examples are known for W,[6e−g] Re,[6h] Co,[6i] and Fe.[6j,8] With regards to iron complexes in particular, 6-coordinate and low-spin,[6n] as well as 5-coordinate and intermediate-spin[6d] $Fe(\eta^1\text{-}N_2H_3)$ species have been characterized. Six-coordinate and low-spin $Fe(\eta^2\text{-}N_2H_3)$ species are also known.[6j,8] Despite the differences in the iron complexes, NMR and structural data suggest that σ-bonding interactions dominate between the iron and hydrazido nitrogen atoms (vide supra). Known examples of iron hydrazido complexes have not exhibited multiple-bond character between the iron and hydrazido nitrogen(s).

As part of our group's ongoing efforts to study the multielectron reactivity of mono- and diiron complexes that feature nitrogenous ligands,[9,10] we recently turned to $(N_2H_x)^{n-}$ (x = 2−4; n = 0, −1, −2) ligated species of iron.[6d,8,11,12] We found that the bridging hydrazine in $\{[PhBP^{Ph}_3]Fe\}_2(\mu\text{-}\eta^1\text{:}\eta^1\text{-}N_2H_4)(\mu\text{-}\eta^2\text{:}\eta^2\text{-}N_2H_2)$ undergoes clean oxidation to diazene, generating $\{[PhBP^{Ph}_3]Fe\}_2(\mu\text{-}\eta^1\text{:}\eta^1\text{-}N_2H_2)(\mu\text{-}\eta^2\text{:}\eta^2\text{-}N_2H_2)$ ($[PhBP^{R}_3]^-$ = $[PhB(CH_2PR_2)_3]^-$) (Scheme 1).[12] Subsequent oxidation results in N_2 loss and formation of

Scheme 1. Oxidation of $\{[PhBP^{Ph}_3]Fe\}_2(\mu\text{-}\eta^1\text{:}\eta^1\text{-}N_2H_4)(\mu\text{-}\eta^2\text{:}\eta^2\text{-}N_2H_2)$

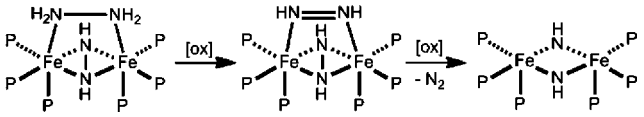

Received: August 2, 2012
Published: September 5, 2012

   dx.doi.org/10.1021/ic301704f | *Inorg. Chem.* 2012, 51, 10043−10054

$\{[PhBP^{Ph}_3]Fe\}_2(\mu\text{-}NH_2)_2$. We wanted to determine if similar transformations could be achieved at monomeric $Fe(N_2H_4)$ and $Fe(N_2H_3)$ species to form monomeric $Fe(N_2H_2)$ and $Fe(N_2H)$ species, respectively.

Herein we report the synthesis, characterization, and subsequent oxidation reactions of a series of monomeric hydrazido and hydrazine complexes of iron(II). These complexes are ligated by a tris(phosphino)borate ligand that is either phenyl or *meta*-terphenyl substituted at the phosphines; the synthesis of the latter ligand scaffold is described. Distinct iron hydrazido species are isolated depending on the nature of the auxiliary ligand employed, including 5-coordinate species that feature multiple-bond character between the iron and the hydrazido ligand. The oxidation of these hydrazido and related hydrazine species of iron is also discussed. In most instances, treatment of these monomeric $Fe(N_2H_x)$ species with oxidizing reagents results in disproportionation of the $(N_2H_x)^{n-}$ ligand, affording $Fe(NH_3)$ species. This reactivity contrasts that observed at diiron centers.[8,11,12]

RESULTS AND DISCUSSION

Synthesis and Characterization of $[PhBP^{mter}_3]$Fe-X Species (X = Cl, Me). To prevent formation of N_2H_x bridging diiron species as discussed above,[8,12] a new, more sterically encumbering $[PhBP^{R}_3]^-$ ligand variant was sought.[13] The incorporation of a bulky terphenyl substituent into a ligand scaffold has successfully been used by others to prepare and stabilize monomeric and/or coordinatively unsaturated metal complexes.[14] Thus, to achieve vertical bulk above the metal center while keeping the steric congestion about the metal similar to that of the related $[PhBP^{Ph}_3]^-$ ligand, the $[PhBP^{mter}_3]^-$ variant was targeted (*m*ter = *meta*-terphenyl = 3,5-terphenyl).

The synthesis of the ligand $[PhBP^{mter}_3]$Tl is readily achieved following a similar synthetic protocol to that employed for $[PhBP^{Ph}_3]$Tl (Scheme 2).[13c,d] The precursor phosphine (*m*-terphenyl)$_2$PMe is prepared in 84% yield by lithium-halogen exchange of *m*-terphenyl bromide with ^{n}BuLi at −78 °C, followed by quenching with half an equivalent of $MePCl_2$. Subsequent deprotonation with ^{s}BuLi at −78 °C in the presence of TMEDA affords the phosphine carbanion, (*m*-terphenyl)$_2$P(CH_2)Li(TMEDA) in 61% yield. Addition of 3 equiv of the carbanion to $PhBCl_2$ and subsequent exposure to 1 equiv of $[Tl](PF_6)$ gives the desired ligand, $[PhBP^{mter}_3]$Tl, which is isolated as a white powder in 62% yield (32% over three steps).[15]

Scheme 2. Synthesis of $[PhBP^{mter}_3]$Tl and $[PhBP^{mter}_3]$Fe-X Species

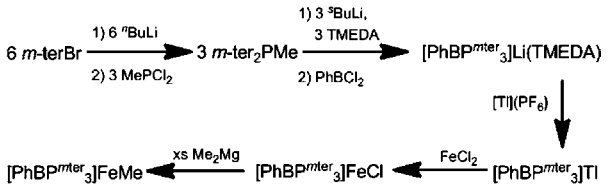

Likewise, the syntheses of the Fe(II) complexes, $[PhBP^{mter}_3]$FeCl and $[PhBP^{mter}_3]$FeMe, are achieved using similar protocols to those used for the syntheses of $[PhBP^{Ph}_3]$FeCl[9b] and $[PhBP^{Ph}_3]$FeMe[12] (Scheme 2). Thus, mixing of $[PhBP^{mter}_3]$Tl with $FeCl_2$ affords yellow and high-spin $[PhBP^{mter}_3]$FeCl (83% yield), and treatment of $[PhBP^{mter}_3]$FeCl with excess Me_2Mg in benzene results in formation of amber and high-spin $[PhBP^{mter}_3]$FeMe (79% yield).

The differences in both the steric and the electronic parameters between the *m*-terphenyl and phenyl substituted ligands can be determined by comparison of the $[PhBP^{R}_3]$FeCl species (R = *m*ter, Ph). The solid-state structures of $[PhBP^{mter}_3]$FeCl and $[PhBP^{Ph}_3]$FeCl[9b] have been obtained, and space-filling renditions are shown in Figure 1. The *m*-terphenyl substituents clearly add vertical protection, as the chlorine atom no longer extends beyond the pocket of the aryl substituents (Figure 1, top). As the *m*-terphenyl substituents are not locked in a rigid position and are free to rotate, the congestion about the iron center is similar in both species (Figure 1, bottom).

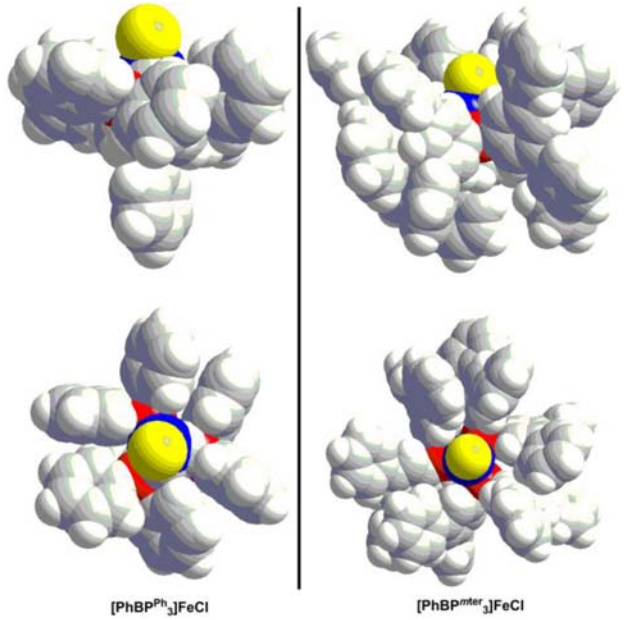

Figure 1. Space filling models of $[PhBP^{Ph}_3]$FeCl (left) and $[PhBP^{mter}_3]$FeCl (right). The representation perpendicular to the B−Fe−Cl vector (top) highlights the added vertical steric protection that the bulkier $[PhBP^{mter}_3]^-$ ligand provides relative to that of the $[PhBP^{Ph}_3]^-$ ligand. The representation parallel to the B−Fe−Cl vector (bottom) indicates that the two ligand scaffolds give a similar level of steric congestion about the iron. Cl are shown in yellow, Fe in blue, P in red, C in gray, H in white, and B in orange.

The cyclic voltammogram (CV) of $[PhBP^{mter}_3]$FeCl features an irreversible reduction at −1.52 V vs Fc/Fc^+ that is very close to the analogous reduction observed in the CV of $[PhBP^{Ph}_3]$FeCl. For comparison, these reductions are about 0.4−0.5 V more positive than those for the alkyl substituted complexes, $[PhBP^{R}_3]$FeCl (R = ^{i}Pr, CH_2Cy).[13a,b] Combined, these studies suggest that the two ligand scaffolds have similar electron-donating capabilities, yet different steric properties.

Synthesis and Characterization of Monomeric Fe(η^2-$N_2R'_3$) Species. An attractive synthetic route to hydrazido species is the direct deprotonation of hydrazine by a metal alkyl species.[6m,12] Indeed, the room temperature addition of 1 equiv of hydrazine to $[PhBP^{mter}_3]$FeMe results in the formation of green and diamagnetic $[PhBP^{mter}_3]$Fe(η^2-N_2H_3) (**1**), with concomitant release of methane (Scheme 3).

The identity of **1** as a hydrazido species is made on the basis of elemental analysis and NMR spectroscopy. The room

dx.doi.org/10.1021/ic301704f | Inorg. Chem. 2012, 51, 10043−10054

Scheme 3. Synthesis of $[PhBP^{mter}_3]Fe(N_2H_3)$ Species

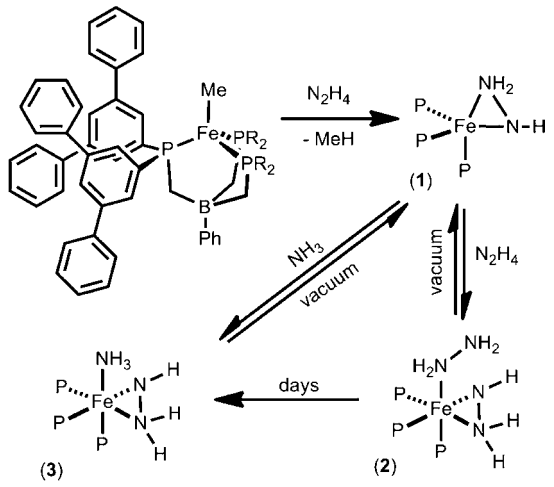

temperature NMR spectra of **1** display broad peaks that sharpen upon cooling to −25 °C, in accordance with an $S = 0$ ground state. The ^{1}H NMR spectrum (−25 °C, THF-d_8) of ^{15}N-**1** (prepared by treatment of $[PhBP^{mter}_3]FeMe$ with $^{15}N_2H_4$) features broad doublets centered at 6.43 (1H) and 3.81 (2H) ppm. In the corresponding ^{15}N NMR spectrum (−25 °C, THF-d_8), the NH_2 nitrogen resonates at −14.5 ppm (dt, $^1J_{NH} \approx 83$ Hz, $^1J_{NN} \approx 11$ Hz), while the *N*H nitrogen resonates at 139.0 ppm (dd, $^1J_{NH} \approx 79$ Hz, $^1J_{NN} \approx 11$ Hz) (Figure 2a). The $^3J_{HH}$ and the $^2J_{NH}$ coupling could not be resolved in either the ^{1}H or the ^{15}N NMR spectra.

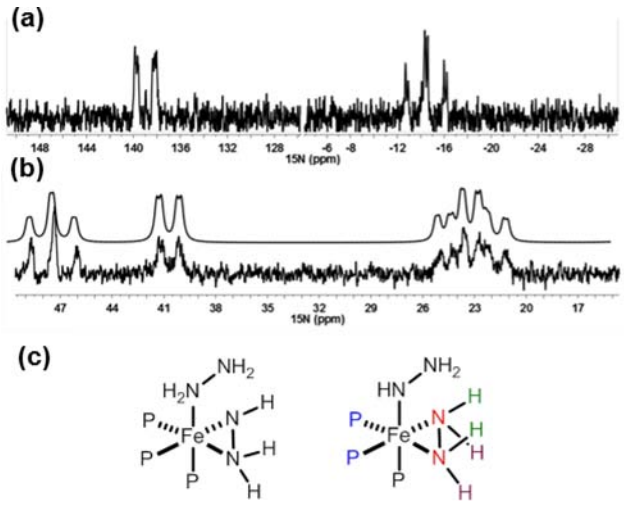

Figure 2. ^{15}N NMR spectra (THF-d_8) of (a): ^{15}**N-1** (−25 °C) and (b): ^{15}**N-2** (−50 °C). The simulation of the spectrum of **2** is shown above the experimental spectrum. Simulation parameters: δ 47.4 ($^1J_{NN}$ = −11 Hz, $^1J_{NH}$ = 65 Hz), 40.6 ($^1J_{NN}$ = −13 Hz, $^1J_{NH}$ = 58 Hz), 23.6 ($^1J_{NN}$ = −11 Hz, $^1J_{NH}$ = 73 Hz, $^1J_{NH}$ = 73 Hz), 22.7 ($^1J_{NN}$ = −13 Hz, $^1J_{NH}$ = 80 Hz, $^1J_{NH}$ = 80 Hz), line width: 15 Hz. (c) Possible isomers of **2**. Equivalent pairs of atoms are shown in color.

The ^{31}P NMR spectrum of **1** (−25 °C, THF-d_8) features a single resonance at 89.1 ppm. The equivalence of the three phosphines suggests that the iron center in **1** is either 4-coordinate and pseudotetrahedral, $[PhBP^{mter}_3]Fe(\eta^1\text{-}N_2H_3)$, or 5-coordinate and fluxional, $[PhBP^{mter}_3]Fe(\eta^2\text{-}N_2H_3)$. As 4-coordinate $[PhBP^{R}_3]Fe^{II}$-X species display high-spin $S = 2$ electronic configurations in the absence of an Fe≡X triple bond linkage,[9b,10,16] **1** is most likely 5-coordinate in solution.

Though hydrazido **1** is stable both in solution and in the solid-state, the open coordination site readily binds L-type ligands. For example, addition of 1 equiv of N_2H_4 or NH_3 to **1** results in a color change from green to orange, and formation of $[PhBP^{mter}_3]Fe(\eta^2\text{-}N_2H_3)(\eta^1\text{-}N_2H_4)$ (**2**) or $[PhBP^{mter}_3]Fe(\eta^2\text{-}N_2H_3)(NH_3)$ (**3**), respectively (Scheme 3). Coordination of either N_2H_4 or NH_3 to **1** is reversible, and exposure of either **2** or **3** to vacuum quantitatively regenerates **1**. Hydrazine/hydrazido **2** is not stable in solution, and over the course of days, hydrazine disproportionation ensues, converting **2** to ammonia/hydrazido **3**, and presumably 0.5 equiv of N_2.

The assignment of **2** as $[PhBP^{mter}_3]Fe(\eta^2\text{-}N_2H_3)(\eta^1\text{-}N_2H_4)$, whereby the hydrazine coordinates end-on and the hydrazido side-on, was made by NMR spectroscopy. Such an isomer should give rise to four distinct ^{15}N NMR resonances, three distinct ^{31}P NMR resonances, and at least six distinct N*H*$_x$ ^{1}H NMR resonances (the asymmetry about the iron center induced by the η^2-N_2H_3 ligand should render the hydrazine $N_\alpha H_2$ inequivalent; Figure 2c left). An alternative assignment of **2**, whereby the hydrazido coordinates end-on and the hydrazine side-on, should give rise to three distinct ^{15}N NMR resonances (the hydrazine nitrogen atoms are now equivalent, vide infra), two distinct ^{31}P NMR resonances, and at most five distinct N*H*$_x$ resonances in the ^{1}H NMR spectrum (Figure 2c right). As the ^{15}N NMR spectrum of ^{15}N-**2** (−50 °C, THF-d_8) features four resonances between 21 and 48 ppm (Figure 2b), **2** must be $[PhBP^{mter}_3]Fe(\eta^2\text{-}N_2H_3)(\eta^1\text{-}N_2H_4)$. Further, the ^{1}H NMR spectrum of ^{15}N-**2** (−50 °C, THF-d_8) features six distinct N*H*$_x$ resonances, and the corresponding ^{31}P NMR spectrum features three distinct resonances.

Select $^1H\{^{15}N\}$ decoupling was employed to correlate the $^{15}N/^1H$ signals (see Supporting Information) allowing for assignment of the hydrazine and hydrazido chemical shifts (Table 1). Briefly, the doublet at 40.6 ppm in the ^{15}N NMR spectrum of ^{15}N-**2** is assigned as the hydrazido *N*H. The triplet centered at 47.4 ppm is assigned as the $N_\beta H_2$ of the coordinated hydrazine, on the basis that (i) select decoupling of this resonance results in collapse of a single NH doublet (that integrates to 2H) in the $^1H\{^{15}N\}$ spectrum, indicating that this NH_2 is not affected by the asymmetry about the iron center, and (ii) the chemical shift is close to that of free hydrazine (ca. 50 ppm under similar conditions, see Supporting Information). The overlapping signals at 22.7 and 23.6 thus correspond to the hydrazine $N_\alpha H_2$ and the hydrazido NH_2; select decoupling of these resonance results in collapse of four NH doublets (1H each) in the $^1H\{^{15}N\}$ spectrum, consistent with the asymmetry about the iron center.

The ^{15}N and ^{1}H NMR chemical shifts for $Fe(\eta^2\text{-}N_2H_x)$ species (x = 2, 3, 4) are summarized in Table 1. Most of these species have ^{15}N NMR chemical shifts that are in the range of free hydrazines and amines, and hence are consistent with sp^3-hybridized nitrogen atoms.[17] For reference, free hydrazine resonates around 50 ppm, and ammonia resonates at 0 ppm.

With the exception of **1**, similar chemical shifts are observed for both types of hydrazido nitrogen atoms (i.e., *N*H and NH_2) for the $Fe(\eta^2\text{-}N_2H_3)$ species. These complexes are all 6-coordinate and low-spin iron(II), and hence similar coordination shifts associated with each ligand type are anticipated.[17] The hydrazido ligand is an LX-type 3 e$^-$ donor, giving rise to an 18-electron iron center. Thus, the low-field chemical shift for the hydrazido *N*H nitrogen atom of **1** is unusual, and suggests a

dx.doi.org/10.1021/ic301704f | Inorg. Chem. 2012, 51, 10043−10054

Table 1. NMR and Structural Parameters for Fe(η^2-N_2H_x) Species (x = 2, 3, 4)

compound	^{15}N NMR chemical shift (δ)[a]	^{1}H NMR chemical shift (δ)	Fe−N bond distance (Å)	ref
{*cis*-[Fe(N_2H_4)(dmpe)$_2$]}{BPh_4}$_2$[d]	−11.9	5.39, 4.69	1.981(2), 2.003(2)	18
{*cis*-[Fe(N_2H_4)(DMeOPrPE)$_2$]}{BPh_4}$_2$[e]	−19.9[b]	4.8, 3.8	1.993(2), 2.006(2)	6j,19
[$PhBP^{Ph}_3$]Fe(Me)(N_2H_4) (**5**)[f]	17.1	4.33, 3.13		this work
{[$PhBP^{Ph}_3$]Fe(NH_3)(N_2H_4)}{PF_6} (**10**)			2.006(2), 2.025(3)	this work
{[$PhBP^{Ph}_3$]Fe(CO)(N_2H_4)}{PF_6} (**13**)		5.48, 2.90	1.984(4), 2.005(3)	this work
{*cis*-[Fe(N_2H_3)(DMeOPrPE)$_2$]}{BPh_4}[g]	8.4/6.1 (*NH*)[b,c] −1.4 (NH_2)[b]	1.05/0.65 (N*H*)[c] 4.23/4.14 (NH*H*)[c] 3.66/3.44 (NH*H*)[c]		6j
[$PhBP^{mter}_3$]Fe(N_2H_3) (**1**)[h]	139.0 (*NH*), −14.5 (NH_2)	6.43 (N*H*), 3.81 (NH_2)		this work
[$PhBP^{mter}_3$]Fe(N_2H_3)(η^1-N_2H_4) (**2**)[i]	40.6 (*NH*), 22.7, 23.6 (NH_2, $N_\alpha H_2$), 47.4 ($N_\beta H_2$)	3.18 (N*H*), 2.52−4.66 (NH_2)		this work
[$PhBP^{mter}_3$]Fe(N_2H_3)(NH_3) (**3**)[j]	31.8 (*NH*), 26.0 (NH_2), −18.9 (NH_3)	1.83 (N*H*), 5.32 (NH*H*), 3.58 (NH*H*), 0.41 (NH_3)	2.003(2) (*Fe*−*NH*) 1.969(2) (*Fe*−NH_2)	this work
[$PhBP^{Ph}_3$]Fe(CO)($NHNH_2$) (**6**)[k]	32.2 (*NH*), 31.8 (NH_2)	2.85 (N*H*), 1.88 (NH*H*), 6.55 (NH*H*)[l]	1.992(3), 2.018(3)	8
[$PhBP^{Ph}_3$]Fe($NHNMe_2$) (**4**)		4.00	1.788(2) (*Fe*−*NH*) 2.058(2) (*Fe*−NMe_2)	this work
cis-[Fe(N_2H_2)(dmpe)$_2$][d]	65.3[b]	2.04	2.016(5), 2.032(7)	18
cis-[Fe(N_2H_2)(DMeOPrPE)$_2$][e]	60.8[b]	2.1		6j

[a]Chemical shifts are referenced to liquid ammonia at 0 ppm. [b]Converted from the nitromethane referencing scale. The chemical shift of nitromethane was taken as 376 ppm relative to liquid ammonia. [c]The two chemical shifts correspond to different isomers. [d]dmpe = 1,2-bis-(dimethylphosphino)ethane. [e]DMeOPrPE = 1,2-bis[(methoxypropyl)phosphino]ethane. [f]NMR collected at −50 °C. [g]NMR collected at −85 °C. [h]NMR collected at −25 °C. [i]NMR collected at −40 °C. [j]NMR collected at −45 °C. [k]NMR collected at −75 °C. [l]Because of H-bonding, the chemical shift of this proton is highly dependent on solvent, concentration, and temperature.

different bonding scenario. The data are consistent with sp^2-hybridization of the hydrazido *N*H, which would allow for the hydrazido to serve as an L$_2$X-type 5 e$^-$ donor. Schrock noted a similar discrepancy in the hydrazido NH/NH_2 resonances of WCp*Me_3(η^2-N_2H_3)$^+$ (*NH*: 241.26 ppm, NH_2: 30.97 ppm),[6e] which has been attributed to formation of a π bond between the hydrazido NH nitrogen and the W center (structural data corroborates this assignment). While such a bonding scenario is typical for M(η^2-N_2R_3) species of the early-to-mid transition metals,[4a,5a,b,e,6e,7c] the high d-electron counts for late transition metals usually preclude this coordination mode; Huttner's d^7 $L_3Co(\eta^2$-$N_2R_3)^+$ species is an exception.[6i]

Though we were unable to obtain crystals of **1** suitable for X-ray diffraction (XRD), the solid-state structure of a related species, [$PhBP^{Ph}_3$]Fe(η^2-NHNMe_2) (**4**), was obtained. This complex is readily prepared by addition of 1 equiv of NH_2NMe_2 to a benzene solution of [$PhBP^{Ph}_3$]FeMe (Scheme 4). On the basis of the similarities between the ^{31}P NMR chemical shifts and the UV−vis spectra of **1** and **4**, the coordination mode of the hydrazido ligand is inferred to be the same in both complexes.

The solid-state structure of **4** is shown in Figure 3. The geometry about the Fe center is best described as distorted trigonal bipyramidal, with P1, P3, and N1 comprising the equatorial plane. The sum of the angles about N1 is 352°, indicating a nearly planar sp^2-hybridized nitrogen atom. The *Fe*-NMe_2 distance of 2.058(2) Å is similar to the Fe−N(sp^3) bond

Scheme 4. Synthesis of [$PhBP^{Ph}_3$]Fe(N_2R_x) Species

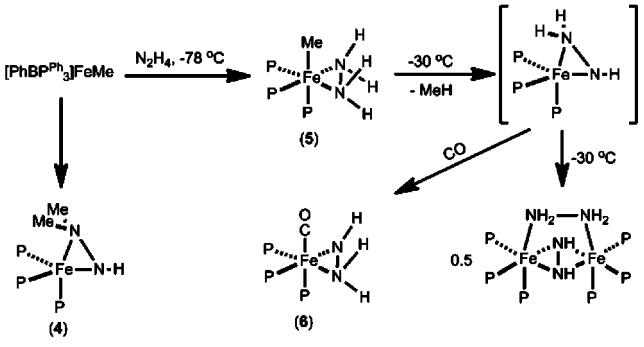

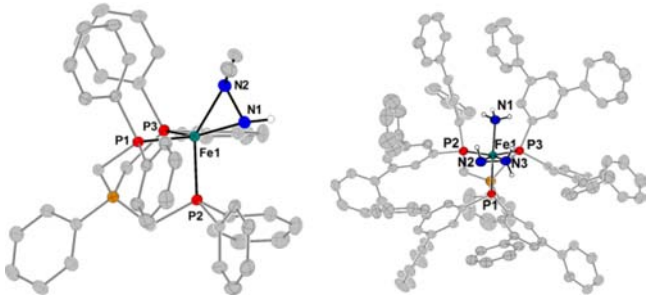

Figure 3. Solid-state structure (50% displacement ellipsoids) of **4** (left) and **3** (right). Most hydrogen atoms, solvent molecules, and minor components of disorder have been removed for clarity. Protons directly coordinated to nitrogen atoms were located in the difference map and are shown. Select bond distances (Å) and angles (deg) for **4**: Fe1−N1 1.788(2), Fe1−N2 2.058(2), Fe1−P1 2.2054(6), Fe1−P2 2.1775(6), Fe1−P3 2.1777(6), N1−N2 1.423(2), N1−Fe1−N2 42.72(6), P1−Fe1−P2 90.52(3), P1−Fe1−P3 91.23(2), P2−Fe1−P3 90.09(3), N1−Fe1−P1 139.71(5), N1−Fe1−P2 147.07(4), N1−Fe1−P3 110.92(5), N2−Fe1−P1 113.16(5), N2−Fe1−P2 147.07(4), N2−Fe1−P3 110.92(5). Select bond distances (Å) and angles (deg) for **3**: Fe1−N1 2.076(2), Fe1−N2 2.003(2), Fe1−N3 1.969(2), Fe1−P1 2.2188(7), Fe1−P2 2.1963(7), Fe1−P3 2.2174(7), N2−N3 1.418(3), N2−Fe1−N3 67.8(1).

dx.doi.org/10.1021/ic301704f | *Inorg. Chem.* 2012, 51, 10043−10054

distances observed in other hydrazido and hydrazine species of iron (Table 1, vide infra), and the *Fe-NH* bond distance of 1.788(2) Å is significantly shorter. For comparison, the average Fe−N bond distance in the low-spin imido species, $[PhBP^{Ph}_3]Fe(NAr)^-$, which features a bona fide Fe≡N triple bond, is 1.6578(2) Å,[9b] and the average Fe−N bond distance in $\{[PhBP^{Ph}_3]Fe(CO)\}_2(\mu\text{-}N_2H_2)$, which features Fe═N bonding, is 1.83 Å.[8] As for **1**, the *Fe−NH* functionality in $\{[PhBP^{Ph}_3]Fe(CO)\}_2(\mu\text{-}N_2H_2)$ lies in the equatorial plane defined by Fe1, P1, and P3, allowing for favorable π-overlap. Thus, the metrical parameters of **1** suggest the presence of an Fe═N bond in **1**.

The solid-state structure of 6-coordinate hydrazido/ammonia **3** was also obtained, and is shown in Figure 3. Though the overall quality of the data set of **3** is compromised by heavily disordered solvent molecules, all of the protons directly coordinated to nitrogen atoms were located in the difference map and were refined semifreely with the aid of distance restraints.[20] The structure clearly establishes the presence of η^2-N_2H_3 and NH_3 ligands coordinating the iron center, with several of the N-coordinated protons engaging in hydrogen bonds to THF solvent molecules that cocrystallize with **3**. The *Fe−NH*$_3$ distance of 2.076(2) Å is consistent with that of other low-spin Fe-NH_3 complexes.[11,21] The similar *Fe−NH* and *Fe−NH*$_2$ distances of 2.003(2) Å and 1.969(2) Å, respectively, are close to those observed in $[PhBP^{Ph}_3]Fe(CO)(\eta^2\text{-}N_2H_3)$,[8] and is in contrast to the disparity in bond distances observed in **4**. Thus, upon coordination of an L-type ligand, the change in geometry from trigonal bipyramidal to octahedral disrupts the Fe═N bonding observed in **1** and **4**. The 18-electron configuration at the iron center is maintained, and now both nitrogen atoms are sp^3-hybridized, and the hydrazido acts as an LX-type ligand.

Synthesis and Characterization of Monomeric Fe-(N_2H_4) Species. In contrast to the reaction between $[PhBP^{mter}]FeMe$ and hydrazine, the room temperature addition of 1 equiv of hydrazine to the sterically less encumbering $[PhBP^{Ph}]FeMe$ species results in quantitative formation of the diiron species $\{[PhBP^{Ph}_3]Fe\}_2(\mu\text{-}\eta^1\text{:}\eta^1\text{-}N_2H_4)(\mu\text{-}\eta^2\text{:}\eta^2\text{-}N_2H_2)$ (Scheme 4).[12] To establish whether this reaction proceeds through an intermediate hydrazido species akin to **1**, the reaction between $[PhBP^{Ph}]FeMe$ and hydrazine was monitored by VT NMR spectroscopy.

Upon addition of hydrazine at −78 °C, an initial hydrazine adduct $[PhBP^{Ph}]Fe(Me)(\eta^2\text{-}N_2H_4)$ (**5**) forms, as ascertained by NMR spectroscopy. The ^{15}N NMR spectrum (−50 °C, THF-d_8) of ^{15}N-**5** displays a single triplet at 17.3 ppm ($^1J_{NH} \approx 76$ Hz), similar to that of other Fe(η^2-N_2H_4) species (Table 1). In the corresponding ^{1}H NMR spectrum of ^{15}N-**5**, a broad singlet corresponding to the Me protons is noted at −0.2 ppm, as well as two broad doublets at 4.33 and 3.13 ppm (2H each, $^1J_{NH} \approx$ 77, 75 Hz, respectively). These resonances correspond to the hydrazine protons that are cis and trans to the Me group, respectively, as determined by a NOESY experiment.

The VT NMR profile of **5** establishes that this species is stable in solution below −30 °C. At this temperature, resonances ascribed to methane and $\{[PhBP^{Ph}_3]Fe\}_2(\mu\text{-}\eta^1\text{:}\eta^1\text{-}N_2H_4)(\mu\text{-}\eta^2\text{:}\eta^2\text{-}N_2H_2)$ begin to grow in. Though the postulated "$[PhBP^{Ph}_3]Fe(N_2H_3)$" species cannot be detected in the ^{1}H or ^{15}N NMR spectra, a single sharp resonance is observed at 84.0 ppm in the ^{31}P NMR spectrum, similar to that of **1** and **4**. Though this species does not appreciably build up in solution, it can be trapped with CO to give $[PhBP^{Ph}_3]Fe(CO)(\eta^2\text{-}N_2H_3)$ (**6**) (Scheme 4).[8]

The synthesis of thermally stable 5- and 6-coordinate iron hydrazine complexes was also explored. Following a similar protocol to that employed by both Tyler[19] and Field,[18] 1 equiv of hydrazine was added to a tetrahydrofuran (THF) solution of $[PhBP^{Ph}_3]FeCl$ in the presence of $[Tl](PF_6)$ to generate $\{[PhBP^{Ph}_3]Fe(\eta^2\text{-}N_2H_4)\}(X)$ (**7**) (X = Cl, PF_6) (Scheme 5).

Scheme 5. Synthesis of $[PhBP^{Ph}_3]Fe(N_2H_4)$ and $\{[PhBP^{CH2Cy}_3]Fe\}_2(\mu\text{-}N_2H_4)$ Species

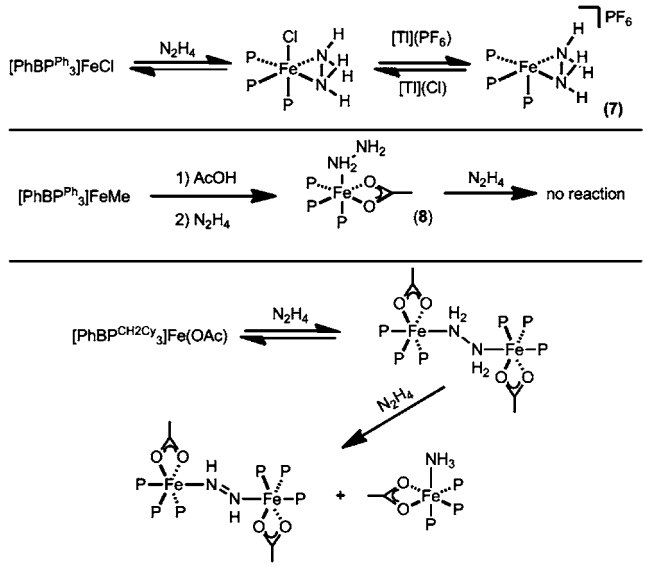

This reaction is hampered by an equilibrium between $[PhBP^{Ph}]FeCl$ and $\{[PhBP^{Ph}_3]Fe(\eta^2\text{-}N_2H_4)\}(X)$. Addition of excess hydrazine or $[Tl](PF_6)$ to the equilibrium mixture results in precipitation of an unidentified but presumably iron containing species and formation of free Ph_2PMe or $[PhBP^{Ph}_3]Tl$, respectively. Similar results were obtained when $[Na](BPh_4)$ was used as the halide abstractor. The hydrazine species **7** could hence not be obtained in analytically pure form, as the chloride and hexafluorophosphate salts cocrystallize. Nonetheless, a structure of **7** has been obtained (see Supporting Information). The disorder present was satisfactorily modeled, and the structure established connectivity and a 5-coordinate square pyramidal geometry for $\{[PhBP^{Ph}_3]Fe(\eta^2\text{-}N_2H_4)\}(PF_6)$.

An end-on coordinated hydrazine species of iron was also targeted. Treatment of $[PhBP^{Ph}_3]FeMe$ with 1 equiv of AcOH, followed by addition of 1 equiv of hydrazine results in clean formation of $[PhBP^{Ph}_3]Fe(OAc)(\eta^1\text{-}N_2H_4)$ (**8**) (Scheme 5). Now, the acetate enforces an end-on coordination of the hydrazine, as shown in the solid-state structure of **8** (Figure 4). This coordination mode is preserved in solution, and two chemical shifts for the hydrazine $N_\alpha H_2$ and $N_\beta H_2$ nitrogen atoms are respectively noted at 33.3 and 56.2 ppm in the ^{15}N NMR spectrum of ^{15}N-**8** (−50 °C, THF-d_8). This assignment is made by analogy to the chemical shifts of the hydrazine ligand noted in **3**, as well as those noted in a related Fe(η^1-N_2H_4) species, in which the N_α nitrogen atom resonates at higher field than the N_β nitrogen atom.[6n] In the corresponding ^{1}H NMR spectrum (−50 °C, THF-d_8), the $N_\alpha H_2$ protons resonate at 4.61 ppm and the $N_\beta H_2$ protons resonate at 3.94 ppm.

dx.doi.org/10.1021/ic301704f | Inorg. Chem. 2012, 51, 10043−10054

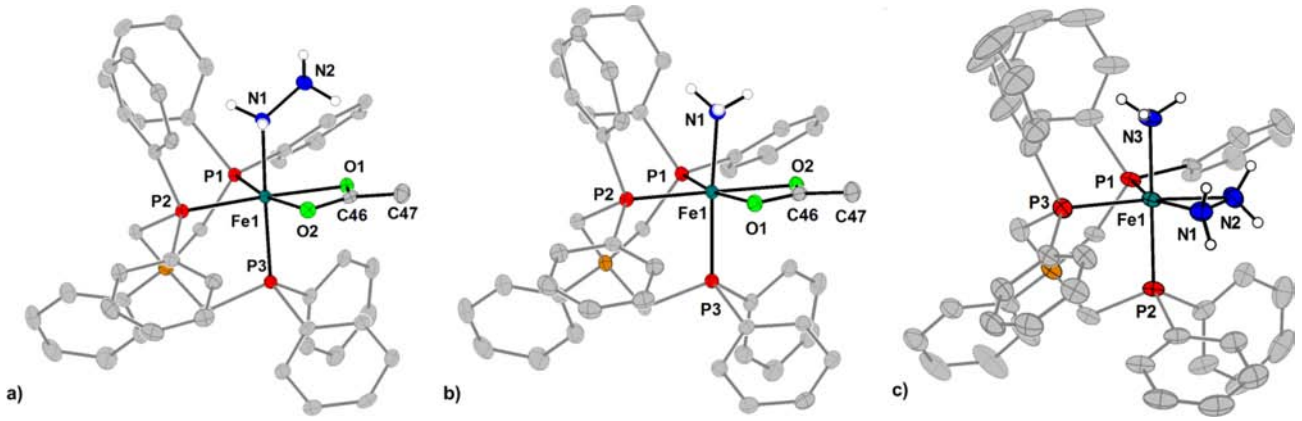

Figure 4. Solid-state structures (50% displacement ellipsoids) of **8** (a), **9** (b), and the cation of **10** (c). Hydrogen atoms, solvent molecules, and minor components of disorder have been removed for clarity. The (PF_6) counteranion of **10** is not shown. The protons directly coordinated to the nitrogen atoms were located in the difference map and are shown. Select bond distances (Å) for **8**: Fe1–N1 2.071(2), N1–N2 1.450(3). Select bond distances (Å) for **9**: Fe1–N1 2.064(1). Select bond distances (Å) and angles (deg) for **10**: Fe1–N1 2.006(2), Fe1–N2 2.025(3), Fe1–N3 2.076(2), N1–N2 1.451(3), N1–Fe1–N2 42.20(9), N1–Fe1–N3 85.14(9), N2–Fe1–N3 86.3(1).

Complex **8** is similar to the diiron species, $\{[PhBP^{CH2Cy}_3]Fe(OAc)\}_2(\mu\text{-}\eta^1\text{:}\eta^1\text{-}N_2H_4)$, which is prepared by addition of hydrazine to the sterically less encumbered $[PhBP^{CH2Cy}_3]Fe(OAc)$ (Scheme 5).[11] Addition of substoichiometric equivalents of hydrazine to $[PhBP^{Ph}_3]Fe(OAc)$ does not result in formation of a hydrazine bridged dimer akin to $\{[PhBP^{CH2Cy}_3]Fe(OAc)\}_2(\mu\text{-}\eta^1\text{:}\eta^1\text{-}N_2H_4)$, suggesting that this species is not accessible for steric reasons. Whereas solutions of **8** are stable toward excess hydrazine, the diiron analogue $\{[PhBP^{CH2Cy}_3]Fe(OAc)\}_2(\mu\text{-}\eta^1\text{:}\eta^1\text{-}N_2H_4)$ facilitates hydrazine disproportionation, and mixtures of $\{[PhBP^{CH2Cy}_3]Fe(OAc)\}_2(\mu\text{-}\eta^1\text{:}\eta^1\text{-}N_2H_2)$ and $[PhBP^{CH2Cy}_3]Fe(OAc)(NH_3)$ are obtained. As hydrazine disproportion is facilitated by electron-rich metal centers,[22] the heightened stability of **8** relative to $\{[PhBP^{CH2Cy}_3]Fe(OAc)\}_2(\mu\text{-}\eta^1\text{:}\eta^1\text{-}N_2H_4)$ towards hydrazine disproportionation is likely due to the hydrazine in **8** coordinating a single iron, and the iron being ligated by a less electron donating tris(phosphino)borate ligand.

Exploring the Oxidation of Hydrazine Species. Diazene coordinated metal species are uncommon, yet are attractive synthetic targets in light of their postulated role in N_2 reduction.[1a,3d] The instability of free diazene precludes its use as a reagent for the direct synthesis of $M(N_2H_2)$ species.[23] Rather, 6-coordinate $M_2(\mu\text{-}\eta^1\text{:}\eta^1\text{-}N_2H_2)$ species (M = Fe,[12,24] Ru,[25] Cr,[26] Mn,[27] Cu[28]) and $M(\eta^1\text{-}N_2H_2)$ species (M = W,[29] Re,[30] Ru,[31] Os[31]) are prepared via oxidation of a coordinated hydrazine ligand. The hydrazine species described above may therefore be expected to serve as precursors to $Fe(\eta^1\text{-}N_2H_2)$ species.[32] In the present system, an alternative reaction occurs, and oxidation results in disproportionation of the $Fe(N_2H_4)$ fragment to give $L_5\text{-}Fe^{II}(NH_3)$ species.

Treatment of 5-coordinate hydrazine **7** with 1 equiv of $Pb(OAc)_4$ results in a color change from pink to purple, and formation of $[PhBP^{Ph}_3]Fe(OAc)(NH_3)$ (**9**) (Scheme 6). Presumably, 0.5 equiv of diazene or N_2 also forms in the reaction. Likewise, treatment of 6-coordinate **8** with $Pb(OAc)_4$ also results in formation of **9**. This species has been characterized by NMR and IR spectroscopies, as well as EA and XRD, and the solid-state structure of **9** is shown in Figure 4.

Hydrazine adduct **5** undergoes a related transformation upon oxidation. As for **7** or **8**, treatment of **5** (−78 °C to room temperature (RT)) with 1 equiv of $Pb(OAc)_4$ results in formation of **9** (Scheme 6). Similarly, in the presence of 1 equiv of N_2H_4, oxidation of **5** by $[Fc](PF_6)$ results in formation of the 6-coordinate ammonia/hydrazine complex, $\{[PhBP^{Ph}_3]Fe(NH_3)(\eta^2\text{-}N_2H_4)\}\{(PF_6)\}$ (**10**). In the absence of N_2H_4, the reaction between **5** and $[Fc](PF_6)$ is ill-defined. As both reactions result in formation of ammonia (and presumably 0.5 equiv of N_2/N_2H_2) the reactions likely proceed via a similar oxidation mechanism. When **5** was instead treated with quinone oxidants, no N-containing Fe products were obtained (see Supporting Information).

Scheme 6. Oxidation of $[PhBP^{Ph}_3]Fe(N_2H_4)$ Species

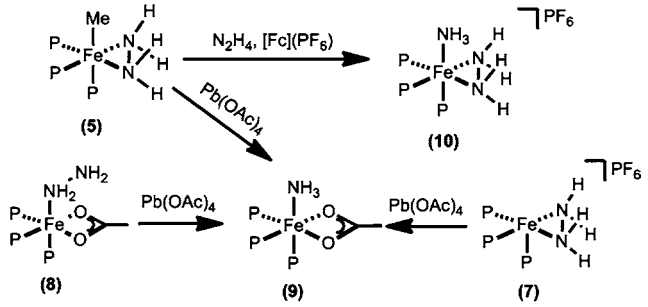

Thus, oxidation of the hydrazine monomers **5**–**7** results in hydrazine disproportionation and isolation of ammonia species **9** or **10** (Scheme 6). The binding mode of the hydrazine/coordination number at iron does not appear to impact the reactivity. This contrasts with the $Pb(OAc)_4$ oxidation of the diiron species $\{[PhBP^{Ph}_3]Fe\}_2(\mu\text{-}\eta^1\text{:}\eta^1\text{-}N_2H_4)(\mu\text{-}\eta^2\text{:}\eta^2\text{-}N_2H_2)$, which results in formation of the diazene species, $\{[PhBP^{Ph}_3]Fe\}_2(\mu\text{-}\eta^1\text{:}\eta^1\text{-}N_2H_2)(\mu\text{-}\eta^2\text{:}\eta^2\text{-}N_2H_2)$ (Scheme 1).

Exploring the Oxidation of Hydrazido Species. Though there are no examples of iron species that are coordinated by the parent diazenido ligand (Fe–N_2H), complexes of the type $Fe(\eta^1\text{-}N_2R)$ can be accessed via alkylation or silylation of a precursor dinitrogen complex $Fe(\eta^1\text{-}N_2R)$,[9g,33] or by deprotonation of a hydrazine species $Fe(\eta^1\text{-}N_2H_3Ph)$ (with concomitant H_2 release).[6d] It is anticipated that hydrazido oxidation may be a viable synthetic route to diazenido species, by analogy to hydrazine oxidation to give diazene species. However, this reactivity is not observed in the present system.

dx.doi.org/10.1021/ic301704f | Inorg. Chem. 2012, 51, 10043–10054

Oxidation of hydrazido species **1** with 1 equiv of $Pb(OAc)_4$ results in a color change from green to purple, and formation of the ammonia complex, $[PhBP^{mter}_3]Fe(OAc)(NH_3)$, (**11**) (Scheme 7). This species is also formed in the reaction of

Scheme 7. Oxidation of $[PhBP^{mter}_3]Fe(N_2H_3)$ Species

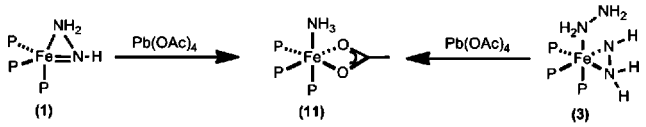

hydrazine/hydrazido **2** with $Pb(OAc)_4$. When **1** or **2** is instead treated with a quinone oxidant, no N-containing iron species are obtained (see Supporting Information).

In contrast to the aforementioned reactivity, in which the coordinated hydrazine or hydrazido ligand is converted to ammonia, no N–N bond cleavage is observed upon oxidation of hydrazido **6** (Scheme 8). When $Pb(OAc)_4$ is added to

Scheme 8. Reactivity of $[PhBP^{Ph}_3]Fe(CO)(N_2H_3)$ Towards Various Oxidants

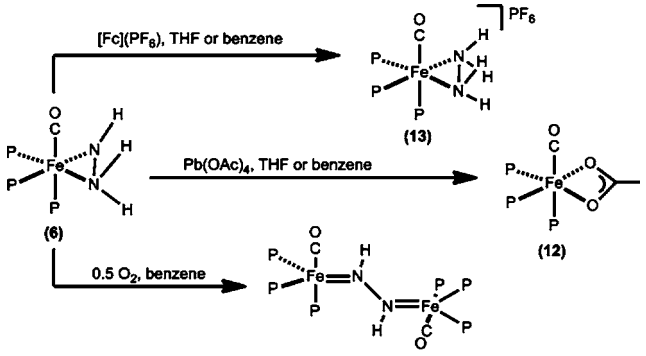

solutions of **6**, no cationic ammonia species akin to **9** or **10** is isolated; rather $[PhBP^{Ph}_3]Fe(CO)(OAc)$ (**12**) forms. When **6** is alternatively treated with 1 equiv of $[Fc](PF_6)$, the cationic hydrazine species $\{[PhBP^{Ph}_3]Fe(CO)(\eta^2\text{-}N_2H_4)\}\{PF_6\}$ (**13**) is cleanly generated along with ferrocene (as deduced by ^1H NMR spectroscopy). Though the net transformation of **6** to **13** is protonation, the formation of ferrocene suggests that the reaction may proceed via an oxidized intermediate, "$[PhBP^{Ph}_3]Fe(CO)(\eta^2\text{-}N_2H_3)^{\bullet+}$", that then abstracts an H-atom from an unknown source to give hydrazine ($H_2NHN\text{–}H$ BDFE(aq) = 83.4 kcal mol^{-1}).[34] The distinct reactivity of **6** relative to **1** or **2** upon oxidation may be due in part to the presence of the carbonyl ligand, which blocks a coordination site and also modulates the electronic structure of the iron center. Curiously, benzene solutions of **6** react with 0.5 equiv of O_2 to generate the diiron species, $\{[PhBP^{Ph}_3]Fe(CO)\}_2(\mu\text{-}\eta^1\text{:}\eta^1\text{-}N_2H_2)$.[8] This reaction does not proceed in THF, which appears to hydrogen bond to a hydrazido proton (deduced by NMR spectroscopy),[8] and may serve to prevent the hydrazido ligand in **6** from engaging in redox and/or acid/base chemistry. The distinct products obtained upon oxidation of **6** underscores the rich redox chemistry of hydrazido species.

CONCLUDING REMARKS

With this report, we have extended our study of the chemistry of hydrazine and hydrazido coordinated iron(II) complexes to include low-spin monomeric species. The coordination chemistry of $N_2H_3^-$ remains relatively scarce, with most examples involving high-valent early metals for both parent and substituted hydrazido ligands. Here we show that when the iron center is in a 6-coordinate environment, the hydrazido ligand acts as an LX-type ligand, with the lone-pair of the sp^3-hybridized NH nitrogen atom not engaging in bonding interactions with the metal. In contrast, in a 5-coordinate environment the iron center adopts a trigonal bipyramidal geometry that allows for Fe=N bonding between the Fe center and an sp^2-hybridized NH nitrogen atom. This latter coordination mode of $N_2R_3^-$ was previously not known for iron and is rare for late transition metals. In the absence of structural data, the coordination mode is readily discernible by ^{15}N NMR spectroscopy; a downfield shift is observed for the sp^2-hybridized *N*R nitrogen relative to the NR_2 nitrogen atom. In contrast, similar ^{15}N NMR chemical shifts are observed for both *N*R and *N*R_2 when both nitrogen atoms of the hydrazido ligand are sp^3-hybridized.

Oxidation of the monomeric iron hydrazine complexes invariably results in disproportionation, and ammonia complexes of iron are isolated. These results contrast with the reactivity that we previously described for a diiron species, whereby oxidation occurs via formal loss of two H-atoms to generate a diazene species.

Similarly, the oxidations of hydrazido species **1** and **2** also result in isolation of an ammonia species. In contrast, the oxidation of carbonyl hydrazido **6** does not yield ammonia; the cationic hydrazine species **13** is isolated upon $[Fc](PF_6)$ oxidation, the carbonyl acetate **12** is isolated upon oxidation with $Pb(OAc)_4$, and the bridging diazene complex $\{[PhBP^{Ph}_3]Fe(CO)\}_2(\mu\text{-}\eta^1\text{:}\eta^1\text{-}N_2H_2)$ is formed upon O_2 oxidation.

Collectively, the diverse reactivity observed upon oxidation of hydrazine and hydrazido ligated iron and diiron species underscores the many redox pathways possible for N_xH_y species.

EXPERIMENTAL SECTION

General Considerations. All manipulations were carried out using standard Schlenk or glovebox techniques under a dinitrogen atmosphere. Glasswear was oven-dried for 12 h (180 °C). Unless otherwise noted, solvents were deoxygenated and dried by sparging with Ar followed by passage through an activated alumina column from S.G. Water (Nashua, N.H.). Nonhalogenated solvents were tested with a standard purple solution of benzophenone ketyl in THF to confirm effective oxygen and moisture removal. Deuterated solvents were purchased from Cambridge Isotopes Laboratories, Inc. and were degassed and stored over activated 3-Å molecular sieves prior to use. Elemental analyses were performed by Midwest Microlab, (Indianapolis, IN) or Complete Analysis Laboratories Inc. (calilabs; Parsippany, NJ).

Electrochemistry. Electrochemical measurements were carried out in a glovebox under a dinitrogen atmosphere in a one-compartment cell using a BAS model 100/W electrochemical analyzer. A glassy carbon electrode and platinum wire were used as the working and auxiliary electrodes, respectively. The reference electrode was Ag/$AgNO_3$ in THF. Solutions (THF) of electrolyte (0.4 M tetra-n-butylammonium hexafluorophosphate) and analyte were also prepared in a glovebox. CVs were externally referenced to Fc/Fc^+.

NMR and IR Spectroscopy. Both Varian 300 and 500 MHz spectrometers were used to record the ^1H NMR and ^{31}P NMR spectra at ambient temperature, and either a Varian 400 or 500 MHz spectrometer was used to record ^{15}N NMR spectra and all VT- NMR spectra. ^1H NMR chemical shifts were referenced to residual solvent, and ^{31}P NMR chemical shifts were referenced to 85% H_3PO_4 at δ 0 ppm. All ^{15}N NMR spectra were externally referenced to neat

dx.doi.org/10.1021/ic301704f | Inorg. Chem. 2012, 51, 10043–10054

$H_3CC^{15}N$ (δ = 245 ppm) in comparison to liquid NH_3 (δ = 0 ppm). Select decoupling experiments were used to correlate ^1H and ^{15}N NMR chemical shifts. All NMR data were worked up using MestReNova. NMR spectral simulation was done with MestReNova. Solution magnetic moments were measured using Evans method.[35] IR measurements were obtained with a KBr solution cell or a KBr pellet using a Bio-Rad Excalibur FTS 3000 spectrometer controlled by Varian Resolutions Pro software set at 4 cm^{-1} resolution.

X-ray Crystallography Procedures. X-ray quality crystals were grown as indicated in the experimental procedures per individual complex. The crystals were mounted on a glass fiber with paratone N oil, and data were collected on a Siemens or Bruker Platform three-circle diffractometer coupled to a Bruker-AXS Smart Apex CCD detector with graphite-monochromated Mo or Cu Kα radiation (λ = 0.71073 or 1.54178 Å, respectively), performing φ-and ω-scans. The structures were solved by direct or Patterson methods using SHELXS[36] and refined against F^2 on all data by full-matrix least-squares with SHELXL-97.[37] All non-hydrogen atoms were refined anisotropically. All hydrogen atoms (except hydrogen atoms on nitrogen) were included into the model at geometrically calculated positions and refined using a riding model. The isotropic displacement parameters of all hydrogen atoms were fixed to 1.2 times the U value of the atoms they are linked to (1.5 times for methyl groups). Hydrogen atoms directly coordinated to nitrogen were located in the Fourier difference map, and refined semifreely with the aid of distance restraints.[20] Expected distances for the type of NH bond at the given temperature were taken from the .lst file.[20] If these hydrogen atoms could not be located in the difference map, they were omitted from the final refinement model.

Some of the structures reported suffered from disorder in parts of the $[PhBP^R_3]^-$ ligand, and the disorder was modeled over two positions. Similarity restraints on 1,2 and 1−3 distances were applied where possible. Similar ADP and rigid bond restraints were applied to all atoms. In addition, several of the structures had solvent disorder, which was modeled as 2 or more component disorder. In some instances, discrete solvent molecules were disordered over several positions, and were modeled using the SUMP command. In other instances, several molecules of solvent were disordered over several positions. To determine the total number of solvent molecules, different free variables were assigned to each partially occupied solvent molecule, and the structure refined. The sum of the free variables was then restrained using the SUMP command to whatever value was obtained without the restraint. Some of the crystals were composed of two or three different species that cocrystallized. $\{[PhBP^{Ph}_3]Fe(N_2H_4)\}(PF_6)$ (**7**), cocrystallized with $\{[PhBP^{Ph}_3]Fe(N_2H_4)(Cl)$ and $[PhBP^{Ph}_3]FeCl$. With the aid of free variables, it was determined that there was a 3% impurity of $[PhBP^{Ph}_3]FeCl$ and 20% $\{[PhBP^{Ph}_3]Fe(N_2H_4)(Cl)$. $[PhBP^{mter}_3]FeCl$ cocrystallized with $[PhBP^{mter}_3]Tl$ (3%). This was modeled with the aid of a free variable (part 1: Fe, Cl, part 2: Tl). All close contacts, both inter and intramolecular, involve at least one partner from a minor component of a disorder. Specific details concerning the refinement of each structure is included in the .cif file.

Starting Materials and Reagents. $[PhBP^{Ph}_3Fe]Me$,[12] **6**,[8] $^{15}NH_2{}^{15}NH_2$,[6e] *meta*-terphenyl bromide,[38] and Me_2Mg[39] were prepared according to literature methods. $Pb(OAc)_4$ was purchased from Aldrich (99.999+%), purified as described in the literature,[40] and recrystallized from cold THF to afford a white crystalline solid. Acetic acid and *para*-benzoquinone were purified according to literature methods.[40] All other reagents were purchased from commercial vendors and used without further purification.

Caution! *All manipulations with anhydrous hydrazine were done at ambient or reduced temperatures, and the waste disposed of appropriately. Anhydrous hydrazine is both highly toxic and highly explosive, with an autoignition temperature that is highly dependent on the presence of impurities. Prior to working with anhydrous hydrazine, we encourage others to consult appropriate sources to familiarize themselves with the dangers. We found "Wiley Guide to Chemical Incompatibilities" (Pohanish, R. P. and Greene, S. A.; Wiley) to be an excellent reference for such matters. Though we did not distill our anhydrous hydrazine, a procedure is described in the literature (Lucien, H. W., J. Chem. Eng. Data, **1962**, 7, 541).*

Synthesis of Complexes. Synthesis of MeP(*m*-terphenyl)$_2$. Terphenyl bromide (8.909 g, 28.81 mmol) was dissolved in 75 mL of THF and chilled to −78 °C. ^{n}BuLi (1.6 M in hexanes, 28.8 mmol) was added dropwise over 15 min, and the reaction was stirred cold for 1 h. In the meantime, $MePCl_2$ (1.736 g, 14.4 mmol) was diluted in 15 mL of toluene and chilled to −78 °C. After 1 h, the phosphine was added dropwise over 10 min to the reaction, which was then stirred for 15 h, slowly warming to RT. The reaction solution was concentrated in vacuo. The resulting residue was washed profusely with petroleum ether, giving cream-colored solids, which were extracted into benzene, filtered through a Celite-lined frit, and lyophilized to afford the desired phosphine (5.765 g, 84% yield). ^1H NMR (C_6D_6, 300 MHz): δ 7.92 (d, J = 6.9 Hz, 4H), 7.73 (s, 2H), 7.46 (d, J = 6.9 Hz, 8H), 7.18−7.11 (m, 12H), 1.56 (d, $^2J_{H-P}$ = 3.6 Hz, 3H, CH_3P). ^{31}P NMR (C_6D_6, 121 MHz): δ −24.2 ppm.

Synthesis of (*m*-terphenyl)$_2$PCH$_2$Li(TMEDA). In a 125 mL Erlenmeyer flask with a stir bar, MeP(*m*-terphenyl)$_2$ (3.7379 g, 7.405 mmol) and TMEDA (1.05 mL, 7.41 mmol) were dissolved in 30 mL of a 2:1 mixture of THF:Et_2O and chilled to −78 °C. ^{s}BuLi (1.4 M in cyclohexane, 8.15 mmol) was added dropwise to the reaction over 10 min. The reaction was stirred for 12 h during which it warmed to room temperature. The resulting red/brown solution was concentrated in vacuo, and the resulting solids were triturated with Et_2O to afford yellow solids which were collected on a frit, and rinsed with Et_2O and pentane. (2.7826 g, 61% yield). ^1H NMR (THF-d_8, 300 MHz): δ 7.92 (d, J = 6.9 Hz, 4H), 7.63 (d, J = 6.9 Hz, 8H), 7.50 (s, 2H), 7.35 (t, J = 6.9 Hz, 8H), 7.23 (t, J = 6.9 Hz, 4H), 2.30 (4H), 2.15 (12H), −0.14 (d, $^2J_{H-P}$ = 3.3 Hz, 2H). ^{31}P NMR (THF, 121 MHz): δ −4.08 ppm.

Synthesis of [PhBP$^{mter}_3$]Tl. In a vial, (*m*-terphenyl)$_2$PCH$_2$Li-(TMEDA) (365.0 mg, 608.6 μmol) was dissolved in 10 mL of Et_2O and then chilled to −90 °C. $PhBCl_2$ (33.2 mg, 202.8 μmol) was diluted in 3 mL of toluene and added dropwise to the solution. The reaction was stirred for 18 h, slowly warming to RT to give $[PhBP^{mter}_3]Li(TMEDA)$ (^{31}P NMR: −10.4 ppm). The reaction was concentrated under reduced pressure to dryness and then suspended in 10 mL of EtOH. $TlPF_6$ (61.1 mg, 202.8 mmol) was added, and the reaction was stirred for 12 h. The white solids in the reaction were collected on a frit and washed with EtOH, MeCN, and petroleum ether (237.1 mg, 62% yield). ^1H NMR (C_6D_6, 500 MHz): δ 8.65 (br d, J = 6.0 Hz, 2H), 7.88−7.85 (m, 13H), 7.68 (t, J = 6.0 Hz, 2H), 7.16−7.13 (overlaps with solvent peak, ∼18H), 7.00−6.99 (overlapping, 48H), 2.77 (br, 6H). ^{31}P NMR (C_6D_6, 121 MHz): δ 21.7 ppm (d, $^1J_{TlP}$ = 4870 Hz). Anal. Calcd. for $C_{117}H_{89}BP_3Tl$: C 77.93; H 4.98; N 0. Found: C 77.85; H 4.86; N 0.

Synthesis of [PhBP$^{mter}_3$]FeCl. $[PhBP^{mter}_3]Tl$ (0.473 g, 0.262 mmol) and $FeCl_2$ (0.034 g, 0.262 mmol) were stirred in 8 mL of THF for 12 h. The reaction was filtered through Celite and concentrated under reduced pressure to dryness. The yellow residue was mashed to a fine powder and washed with petroleum ether and Et_2O (0.369 g, 83%). Single crystals suitable for X-ray diffraction were grown from vapor diffusion of petroleum ether into a benzene solution of $[PhBP^{mter}_3]FeCl$. ^1H NMR (C_6D_6, 300 MHz): δ 206.1 (s), 40.9 (s), 19.8 (s), 18.4 (s), 7.1 (s), 6.9 (s), 3.6 (s), −14.3 (s), −37.3 (s). Evans Method (C_6D_6): 5.32 μ_B Anal. Calcd. for $C_{117}H_{89}BClFeP_3$: C 83.15; H 5.31; N 0. Found: C 83.09; H 5.41; N 0.

Synthesis of [PhBP$^{mter}_3$]FeMe. A solution of $[PhBP^{mter}_3]FeCl$ (0.2096 g, 0.141 mmol) in 15 mL of benzene was added to a stirring slurry of Me_2Mg (0.0186 g, 0.342 mmol) in 2 mL of benzene. After stirring for an hour, the reaction was filtered through a Celite-lined frit, and the solution was lyophilized to dryness. The residue was extracted into 20 mL of benzene, filtered through a Celite-lined frit, and again lyophilized to yield analytically pure $[PhBP^{mter}_3]FeMe$ (0.1629 g, 78.8%). ^1H NMR (C_6D_6, 300 MHz): δ 46.1 (s), 22.0 (s), 20.3 (s), 6.8 (s), 6.6 (s), 1.7 (s), −13.5 (s), −49.8 (s). Evans Method (C_6D_6): 4.9 μ_B UV−vis (C_6H_6) λ_{max}, nm (ε, M^{-1} cm^{-1}): 405 (1750), 370 (2300). Anal. Calcd. for $C_{118}H_{92}BFeP_3$: C 84.88; H 5.55. Found: C 84.67; H 5.62.

dx.doi.org/10.1021/ic301704f | Inorg. Chem. 2012, 51, 10043−10054

Synthesis of [PhBP$^{Ph}_3$]Fe(OAc). Neat acetic acid (29.5 μL, 0.515 mmol) was added to a solution of [PhBP$^{Ph}_3$]FeMe (0.3892 g, 0.515 mmol) in 18 mL of THF. After stirring for 24 h, the volatiles were removed to afford pure material. Crystals suitable for XRD were grown from benzene/pentane. ^{1}H NMR (C_6D_6, 300 MHz): δ 171 (bs), 130.0 (s), 30.1 (s), 16.0 (s), 14.8 (s), −7.1 (s), −26.4 (s). Evans Method (C_6D_6): 4.6 μ_B Anal. Calcd. for $C_{47}H_{44}BFeO_2P_3$: C 70.52; H 5.74; N 0. Found: C 71.85; H 5.74; N 0.

Synthesis of [PhBP$^{mter}_3$]Fe(η^2-N$_2$H$_3$), 1. [PhBP$^{mter}_3$]FeMe (0.0318 g, 0.0217 mmol) was dissolved in 2 mL of THF, and a solution of hydrazine (0.77 μL, 0.0217 mmol) in 1 mL of THF was added dropwise. The stirring reaction immediately changed color from yellow to green, and **1** was quantitatively formed. Microcrystals of **1** were grown by slow evaporation of pentane into a THF solution (16.1 mg, 50.0%). Complex **1** displays broad NMR spectra at all temperatures, and −25 °C was found to give the sharpest spectra. ^{1}H NMR (THF-d_8, 500 MHz, −25 °C): δ 6.75−8.20 (bm, 83H), 6.43 (s, 1H, NH), 3.81 (s, 2H, NH_2). 1.79 (m, 6H, CH_2, overlapping with THF). ^{31}P NMR (THF-d_8, 202.3 MHz, −25 °C): δ 89.1. IR (KBr) (cm^{-1}): 3301, 3174. UV−vis (THF) λ_{max}, nm (ε, M^{-1} cm^{-1}): 348 (sh, 4900), 420 (sh, 1600), 605 (625), 708 (500). Anal. Calcd. for $C_{117}H_{92}BFeN_2P_3$: C 83.36; H 5.50; N 1.66. Found: C 82.97; H 5.76; N 1.55.

A sample of 95% ^{15}N-enriched **1** was synthesized using an analogous synthetic procedure with $^{15}NH_2{}^{15}NH_2$. ^{1}H NMR (THF-d_8, 500 MHz, −25 °C): δ 6.43 (d, $^1J_{NH}$ ≈ 79 Hz, 1H, NH), 3.81 (d, $^1J_{NH}$ ≈ 83 Hz, 2H, NH_2). ^{15}N NMR (THF-d_8, 50.7 MHz, −25 °C): δ 139.0 (dd, $^1J_{NH}$ ≈ 78.6 Hz, $^1J_{NN}$ ≈ 11 Hz), −14.5 (dt, $^1J_{NH}$ ≈ 83 Hz, $^1J_{NN}$ ≈ 11 Hz).

Synthesis of [PhBP$^{mter}_3$]Fe(η^2-N$_2$H$_3$)(η^1-N$_2$H$_4$), 2. [PhBP$^{mter}_3$]$^-$FeMe (0.0269 g, 0.0184 mmol) was dissolved in 2 mL of THF, and a solution of hydrazine (3.0 μL, 0.092 mmol) in 1 mL of THF was added dropwise. The stirring reaction immediately changed color from yellow to green to red, indicative of formation of **2**. Microcrystals of **3** can be grown by evaporation of pentane into a THF solution containing **2** and excess hydrazine (11.4 mg, 36.2%). The coordinated hydrazine is labile, and exposure of **2** to vacuum results in formation of **2**. EA was performed on crystals of **3** (grown from THF/pentane) that were dried under an N_2 atmosphere for 20 min prior to sealing in an ampule, and it thus is likely that THF or pentane is still present in the crystals. Anal. Calcd. for $C_{117}H_{96}BFeN_4P_3$: C 81.77; H 5.63; N 3.26. Anal. Calcd. for [PhBP$^{mter}_3$]Fe(η^2-N$_2$H$_3$)(η^1-N$_2$H$_4$).5THF, $C_{137}H_{136}BFeN_4P_3O_5$: C 79.18; H 6.60; N 2.70 Found: C 78.95; H 6.16; N 3.09. ^{1}H NMR (THF-d_8, 500 MHz, −40 °C): δ 9.90 (s, 1H), 8.38 (m, 6H), 6.7−8.1 (m, 76H), 4.92 (s, 1H, NH_2 or $N_\alpha H_2$), 4.66 (s, 2H, $N_\beta H_2$), 3.18 (s, 1H, NH_2 or $N_\alpha H_2$), 2.91 (s, 1H, NH_2 or $N_\alpha H_2$), 2.72 (s, 1H, NH), 2.52 (s, 1H, NH_2 or $N_\alpha H_2$), 2.18 (m, 2H, CH_2), 1.20 (m, 4H, CH_2). ^{31}P NMR (THF-d_8, 202.3 MHz, −40 °C): δ 76.45 (d, 1P, J ≈ 40 Hz), 73.25 (bs, 1P), 59.58 (d, 1P, J ≈ 66 Hz). The ^{31}P coupling was ill-defined at all temperatures scanned. IR (KBr) (cm^{-1}): 3305, 3170. UV−vis (THF, with 20 equiv of N_2H_4) λ_{max}, nm (ε, M^{-1} cm^{-1}): 383 (2600, sh), 512 (1280).

A sample of 95% ^{15}N-enriched **2** was synthesized using an analogous synthetic procedure with $^{15}NH_2{}^{15}NH_2$. ^{1}H NMR (THF-d_8, 500 MHz, −40 °C): δ 4.92 (d, $^1J_{NH}$ ≈ 80 Hz 1H, NH_2 or $N_\alpha H_2$), 4.66 (d, $^1J_{NH}$ ≈ 65 Hz, 2H, $N_\alpha H_2$), 3.18 (d, $^1J_{NH}$ ≈ 75 Hz 1H, NH_2 or $N_\alpha H_2$), 2.91 (d, $^1J_{NH}$ ≈ 75 Hz, 1H, NH_2 or $N_\alpha H_2$), 2.72 (d, $^1J_{NH}$ ≈ 60 Hz, 1H, NH), 2.52 (d, $^1J_{NH}$ ≈ 80 Hz, 1H, NH_2 or $N_\alpha H_2$). ^{15}N NMR (THF-d_8, 50.7 MHz, −40 °C): 47.4 (dt, $N_\beta H_2$, $^1J_{NH}$ ≈ 65 Hz, $^1J_{NN}$ = −11 Hz), 40.6 (dd, NH, $^1J_{NH}$ ≈ 58 Hz, $^1J_{NN}$ = −13 Hz), 23.6 (dt, NH_2 or $N_\alpha H_2$, $^1J_{NH}$ ≈ 73 Hz, $^1J_{NN}$ = −11 Hz), 22.7 (dt, NH_2 or $N_\beta H_2$, $^1J_{NH}$ ≈ 80 Hz, $^1J_{NN}$ = −13 Hz). Select ^{1}H{^{15}N} decoupling was employed to confirm the HN connectivity.

Synthesis of [PhBP$^{mter}_3$]Fe(η^2-N$_2$H$_3$)(NH$_3$), 3. A solution of **1** (0.0150 g, 0.00890 mmol) in 1 mL of THF was transferred to a 15 mL Shlenk tube, and evacuated. One atm of NH_3 was added, and the solution immediately turned red. Slow evaporation of pentane into a THF solution of **3** afforded crystalline material (0.0122 g, 80.5%). Exposure of either solutions of **3** or crystals of **3** to vacuum resulted in rapid reformation of **1**. Upon removal of solvent, crystals of **3** rapidly changed color to green and hence satisfactory EA could not be obtained. ^{1}H NMR (THF- d_8, 400 MHz, −45 °C): δ 10.3 (s, 1H), 8.66 (s, 1H), 8.53 (s, 1H), 8.22 (s, 2H), 8.08 (s, 2H), 6.5−8.1 (m, 76H), 5.32 (s, 1H), 3.58 (s, 1H, overlapping with THF), 2.6 (s, 2H), 2.2 (s, 2H), 1.83 (s, 1H, overlapping with solvent), 1.5 (s, 2H), 0.41 (s, 3H, overlapping with residual NH_3). ^{31}P NMR (THF-d_8, 162 MHz, −45 °C): δ 81.1 (d, 1P, J ≈ 48 Hz), 66.2 (d, 1P, J ≈ 67 Hz), 52.3 (m, 1P). The ^{31}P coupling was ill-defined at all temperatures scanned (20 °C to −70 °C). IR (KBr) (cm^{-1}): 3245, 3198. UV−vis (THF, under 1 atm NH_3) λ_{max}, nm (ε, M^{-1} cm^{-1}): 400 (2900, sh), 516 (1460).

A sample of 95% ^{15}N-enriched **3** was synthesized using an analogous synthetic procedure with $^{15}NH_2{}^{15}NH_2$. ^{1}H NMR THF-d_8, 400 MHz, −45 °C): δ 5.32 (d, $^1J_{NH}$ ≈ 82 Hz, 1H, N*H*H), 3.58 (d, 1H, NH*H*), 1.83 (1H, N*H*), 0.41 (d, $^1J_{NH}$ ≈ 60 Hz, 3H, NH_3). gHMQC ^{15}N{^{1}H} NMR (THF-d_8, 40.5 MHz, −45 °C): δ 31.8 (*N*H), 26.0 (*N*H_2), −18.9 (*N*H_3). Select ^{1}H{^{15}N} decoupling was employed to confirm the HN connectivity.

Synthesis of [PhBP$^{Ph}_3$]Fe(η^2-NHNMe$_2$), 4. Neat NH_2NMe_2 (28.2 μL, 0.363 mmol) was added to a stirring solution of [PhBP$^{Ph}_3$]FeMe (0.2495 g, 0.3299 mmol) in 10 mL of benzene. The reaction was heated to 50 °C for 48 h, during which time the color changed from yellow to green. The volatiles were removed to afford a green solid (0.2356 g, 89.5%). Crystals suitable for XRD were grown from the slow evaporation of pentane into a saturated benzene solution of **4**. ^{1}H NMR (C_6D_6, 300 MHz): δ 8.13 (d, 2H, J = 6 Hz), 7.64 (t, 2H, J = 6 Hz), 7.40 (t, 1H, J = 6 Hz), 7.31 (bs, 12H), 6.88 (t, 6H, J = 7 Hz), 6.76 (t, 12H, J = 7 Hz), 4.00 (s, 1H, NH), 2.16 (s, 6H, NMe_2), 1.63 (bs, 6H, CH_2). ^{31}P NMR (C_6D_6, 121.4 MHz): δ 79.9. IR (KBr) (cm^{-1}): 3234. UV−vis (THF) λ_{max}, nm (ε, M^{-1} cm^{-1}): 300 (sh, 8450), 340 (sh, 4400), 440 (700), 600 (466), 742 (320). Anal. Calcd. for $C_{47}H_{48}BFeN_2P_3$: C 70.52; H 6.04; N 3.50. Found: C 69.97; H 6.14; N 3.18.

Synthesis of [PhBP$^{Ph}_3$]Fe(Me)(η^2-N$_2$H$_4$), 5. [PhBP$^{Ph}_3$]FeMe (0.0343 g, 0.0391 mmol) was dissolved in 500 μL of THF, and stirred at −78 °C. To this, a solution of hydrazine (1.27 μL, 0.0391 mmol) dissolved in 280 μL of THF was added dropwise, resulting in a color change from yellow to strawberry red and conversion to **5**. ^{1}H NMR (THF-d_8, 500 MHz, −50 °C): δ 7.56 (bs, 7H), 7.27 (m, 2H), 7.19 (m, 4H), 7.12 (m, 2H), 6.97 (m, 4H), 6.89 (bs, 8H), 6.74 (m, 8H), 4.33 (s, 2H, NH_{cis}H), 3.13 (s, 2H, NHH_{trans}), 1.30 (m, 6H, CH_2), −0.2 (s, 3H, Me). NOESY was employed to assign the hydrazine protons that are cis and trans to the methyl ligand. ^{31}P NMR (THF-d_8, 202.3 MHz, −50 °C): δ 79.18 (d, 2P, J ≈ 28 Hz), 52.50 (t, 1P, J = 32.1 Hz). The doublet is broad and not well-resolved. UV−vis (THF, −78 °C) λ_{max}, nm (ε, M^{-1} cm^{-1}): 524 (940). IR (THF/KBr, −78 °C) (cm^{-1}): 3302, 3246, 3161.

A sample of 95% ^{15}N-enriched **5** was synthesized using an analogous synthetic procedure with $^{15}NH_2{}^{15}NH_2$. ^{1}H NMR (THF-d_8, 500 MHz, −50 °C): δ 4.31 (d, $^1J_{NH}$ ≈ 77 Hz, 1.5H, NH_{cis}H), 3.12 (d, $^1J_{NH}$ ≈ 75 Hz, 1.5H, NHH_{trans}). ^{15}N NMR (THF-d_8, 50.7 MHz, −50 °C): δ 17.3 (t, $^1J_{NH}$ ≈ 76 Hz, 2N). IR (THF/KBr, −78 °C) (cm^{-1}): 3312, 3251, 3223.

Synthesis of {[PhBP$^{Ph}_3$]Fe(η^2-N$_2$H$_4$)}(PF$_6$), 7. To a solution of PhBP$^{Ph}_3$FeCl (0.6023 g, 0.775 mmol) in 20 mL of THF was added neat hydrazine (37.7 μL, 1.16 mmol) and solid [Tl](PF$_6$) (0.2764 g, 0.775 mmol). After stirring for 24 h, hydrazine was again added (12.2 μL, 0.39 mmol), and the reaction stirred an additional 24 h. The solution was filtered through Celite, and the volatiles removed. The solid was extracted into DME, filtered through a Celite-lined frit, and the volatiles removed to give 0.6739 g of a pink solid (95%). Crystals suitable for X-ray diffraction were grown from a THF/pentane solution. ^{1}H NMR (THF-d_8, 500 MHz, −20 °C): δ 7.8 (m, 3H), 7.58 (d, J = 7.50 Hz, 2H), 7.44 (m, 3H), 7.38 (m, 3H), 7.19 (m, 5H), 7.12 (t, J = 7.54 Hz, 4H), 7.08 (t, J = 6.70, 2H), 7.00 (m, 5H), 6.83 (t, J = 7.54 Hz, 4H), 6.78 (J = 7.54 Hz, 4H), 4.78 (bs, NH_2, 2H), 4.31 (bs, NH_2, 2H), 1.30 (d, CH_2, $^2J_{HP}$ ≈ 15 Hz, 6H). ^{31}P NMR (THF-d_8, 202.3 MHz, −20 °C): δ 66.0 (d, J = 59.3 Hz, 2P), 58.9 (t, J = 59.3 Hz, 1P), −138.6 (m, 1P). IR (KBr) (cm^{-1}): 3335, 3281, 3143. UV−vis (THF) λ_{max}, nm (ε, M^{-1} cm^{-1}): 420 (250), 525 (675). Crystals of **7** invariable contained {[PhBP$^{Ph}_3$]Fe(η^2-N$_2$H$_4$)}(PF$_6$), [PhBP$^{Ph}_3$]FeCl,

dx.doi.org/10.1021/ic301704f | Inorg. Chem. 2012, 51, 10043−10054

and {[PhBP$^{Ph}_3$]Fe(η^2-N_2H_4)}(Cl), precluding our ability to obtain analytically pure material.

Synthesis of [PhBP$^{Ph}_3$]Fe(η^1-N_2H_4)(OAc), 8. Neat anhydrous hydrazine (10.2 μL, 0.3159 mmol) was added to a 2 mL THF solution of [PhBP$^{Ph}_3$]Fe(OAc) (0.2529 g, 0.3159 mmol). An immediate color change from pale yellow to purple was noted. After stirring for 24 h, the reaction was filtered, and solid **8** was rinsed with THF and pentane to afford analytically pure material (0.1920 g, 73%). Crystals suitable for diffraction were grown by layering a saturated benzene solution of **8** with pentane. ^{1}H NMR (THF-d_8, 500 MHz, −50 °C): δ 6.5−8.0 (m, 35H), 4.61 (bs, NH_2, 2H), 3.94 (bs, NH_2, 2H), 1.5−1.8 (m, 3H, overlapping with THF), 1.5−1.8 (m, 6H) ^{31}P NMR (THF-d_8, 202.3 MHz, −50 °C): δ 59.1 (bs, 2P), 50.5 (t, J = 57.0 Hz, 1P). IR (KBr) (cm^{-1}): 3378, 3313, 1464. Anal. Calcd. for $C_{47}H_{48}BFeP_3N_2O_2$: C 67.81; H 5.81; N 3.36. Found: C 67.43; H 5.62; N 3.06.

A sample of 95% ^{15}N-enriched **8** was synthesized using an analogous synthetic procedure with $^{15}NH_2{}^{15}NH_2$. ^{1}H NMR (THF-d_8, 500 MHz, −50 °C): δ 4.61 (d, $^1J_{NH}$ = 70 Hz, 2H, N$_\alpha$H$_2$), 3.94 (d, $^1J_{NH}$ = 67 Hz, 2H, N$_\beta$H$_2$). ^{15}N NMR (THF-d_8, 50.7 MHz, −50 °C): δ 56.2 (t, $^1J_{NH}$ = 67 Hz, 1N, N$_\beta$H$_2$), 33.3 (t, $^1J_{NH}$ = 68 Hz, 1N, N$_\alpha$H$_2$). ^{1}H{^{15}N} experiments with selective decoupling were used to correlate the ^{1}H and ^{15}N NMR chemical shifts. IR (KBr) (cm^{-1}): 3367, 3300, 3274.

Complex **8** can alternatively be prepared from the salt metathesis of **7** with sodium acetate.

Synthesis of [PhBP$^{Ph}_3$]Fe(NH$_3$)(OAc), 9. A suspension of Pb(OAc)$_4$ (0.0161 g, 0.0360 mmol) in 1 mL of THF was added dropwise to a stirring solution of **7** (36.0 mg, 0.036 mmol) in 2 mL of THF. The reaction gradually changed color from pink to purple, as Pb(OAc)$_2$ precipitated out. The volatiles were removed, and the solid residue was extracted into benzene, and filtered through a Celite-lined frit. The solution was lyophilized, extracted into benzene, and again filtered through a Celite-lined frit. Crystals were grown by layering pentane over the benzene solution (10.3 mg, 35.5%). Complex **9** is sparingly soluble and crystals of **8** are invariably covered with a white film, presumably Pb(OAc)$_2$.

Complex **9** can alternatively be prepared by addition of 1 atm of NH$_3$ to a solution of [PhBP$^{Ph}_3$]Fe(OAc) (0.0284 g, 0.0355 mmol) in 4 mL of benzene (in an evacuated 50 mL Schlenk-tube). After stirring for 5 min, the solution was degassed, filtered through Celite, and layered with pentane to afford crystalline material (0.0211 g, 72.7%). ^{1}H NMR (THF-d_8, 500 MHz, −40 °C): δ 7.75 (bs, 5H), 7.51 (d, J = 6.9 Hz, 4H), 7.38 (m, 5H), 7.24 (m, 3H), 6.9−7.2 (m, 15H), 6.83 (m, 3H), 2.36 (s, 3H, NH$_3$), 0.95−1.40 (m, 9H, CH$_2$/OAc). ^{31}P NMR (d_8-THF, 202.3 MHz, −40 °C): δ 61.5 (bs, 2P), 46.9 (t, J = 58.6 Hz, 1P). IR (KBr) (cm^{-1}): 3362, 3334, 1466. UV−vis (THF) λ_{max}, nm (ε, M^{-1} cm^{-1}): 580 (855).

Crystals of **9** were exposed to minimal vacuum prior to sealing in an ampule/combustion analysis. Anal. Calcd. for $C_{47}H_{47}BFeP_3NO_2$: C 69.05; H 5.80; N 1.71. Anal. Calcd. for [PhBP$^{Ph}_3$]Fe(NH$_3$)(OAc).C_6H_6, $C_{53}H_{53}BFeP_3NO_2$: C 71.10; H 5.96; N 1.56. Found: C 70.70; H 6.06; N 1.50.

A sample of 95% ^{15}N-enriched **9** was synthesized following the alternative procedure, using ^{15}NH$_3$. ^{1}H NMR (THF-d_8, 400 MHz, −30 °C): δ 2.36 (d, $^1J_{NH}$ = 67 Hz, 3H, NH$_3$). HSQC ^{15}N{^{1}H} NMR (THF-d_8, 40.5 MHz, −30 °C): δ −13.8. ^{31}P NMR (THF-d_8, 161.8 MHz, −40 °C): δ 61.5 (bs, 2P), 46.9 (dt, $^1J_{PP} \approx$ 58.6 Hz, $^1J_{NP} \approx$ 10 Hz, 1P). IR (KBr) (cm^{-1}): 3354, 3327, 1466.

Synthesis of {[PhBP$^{Ph}_3$]Fe(η^2-N_2H_4)(NH$_3$)}(PF$_6$), 10. A solution of [PhBP$^{Ph}_3$]FeMe (0.2181 g, 0.2883 mmol) in 15 mL of THF was cooled to −41 °C and set stirring. To this, a solution of hydrazine (18.7 μL, 0.577 mmol) in 1 mL of THF was added dropwise over the course of 5 min. A suspension of [Fc](PF$_6$) (0.0954 g, 0.2883 mmol) in 4 mL of THF was added dropwise, and the reaction was stirred for 1 h at −41 °C, and subsequently warmed to RT and stirred an additional 12 h. Volatiles were removed from the reaction mixture, and the pink residue was rinsed with 15 mL of pentane, followed by 10 mL of Et$_2$O. Extraction of the remaining solid into THF, followed by layering with pentane, afforded crystals of **10** (0.1887 g, 70.0%). ^{1}H NMR (THF-d_8, 300 MHz): δ 6.5−8.5 (m, 35H), 5.5 (bs, NH_2, 2H), 4.2 (bs, NH_2, 2H), 2.7 (bs, NH_3, 3H), 1.37 (m, CH$_2$, 6H) ^{31}P NMR (THF-d_8, 300 MHz): δ 60.8 (bs, 2P), 53.5 (bs, 1P), −143.3 (m, 1P). IR (KBr) (cm^{-1}): 3334 (NH), 3260 (NH). UV−vis (THF) λ_{max}, nm (ε, M^{-1} cm^{-1}): 537 (750). Anal. Calcd. for $C_{45}H_{48}BFeN_3P_4F_6$: C 57.78; H 5.17; N 4.49. Found: C 57.85; H 5.25; N 4.29.

Synthesis of [PhBP$^{mter}_3$]Fe(NH$_3$)(OAc), 11. Hydrazine (6.4 μL, 0.020 mmol) was added to a stirring solution of [PhBP$^{mter}_3$]FeMe (0.1439 g, 0.0982 mmol) in 5 mL of THF. After stirring for 10 min, a suspension of Pb(OAc)$_4$ (0.0871 g, 0.0196 mmol) in 5 mL of THF was added dropwise, and the solution stirred for 12 h. The volatiles were removed, and the resulting residue was rinsed with pentane and extracted into DME. The resulting solution was layered with pentane to yield crystalline **10** (0.0803 g, 53.6%). The bulk crystals contained a white precipitate, presumably Pb(OAc)$_2$.

Complex **11** can alternatively be prepared from [PhBP$^{mter}_3$]FeMe. One equivalent of AcOH (2.4 μL, 0.041 mmol) was added to a solution of [PhBP$^{mter}_3$]FeMe (0.0686 g, 0.0411 mmol) in 2 mL of benzene. After stirring for 10 min, the reaction was transferred to a 5 mL Schlenk tube which was evacuated. One atmosphere of NH$_3$ was added to the Schlenk tube, and after stirring for 1 h, the reaction was degassed, the solution filtered through Celite, and layered with pentane to afford crystalline material (0.0444 g, 62.4%).

^{1}H NMR (THF-d_8, 400 MHz, −30 °C): δ 8.7 (bs, 6H), 7.6−8.4 (m, 7H), 6.8−8.4(m, 70H), 3.05 (bs, NH_3, 3H), 1.5−2.0 (m, 6H, overlap with THF), 1.29 (s, 3H, OAc). ^{31}P NMR (THF-d_8, 161.8 MHz, −30 °C): δ 60.7 (bs, 2P), 50.1 (t, J = 59.4 Hz, 1P), −143.3 (m, 1P). IR (KBr) (cm^{-1}): 3365, 1450. UV−vis (THF) λ_{max}, nm (ε, M^{-1} cm^{-1}): 557 (580). Anal. Calcd. for $C_{119}H_{95}BFeNO_2P_3$: C 82.58; H 5.53; N 0.81. Found: C 81.25; H 5.98; N 0.84.

A sample of 95% ^{15}N-enriched **11** was synthesized using the alternative synthesis using ^{15}NH$_3$. ^{1}H NMR (THF-d_8, 400 MHz, −30 °C): δ 3.05 (d, $^1J_{NH}$ = 67 Hz, 3H, NH$_3$). HSQC ^{15}N{^{1}H} NMR (THF-d_8, 40.5 MHz, −30 °C): δ −12.7. IR (KBr) (cm^{-1}): 3308 (NH), 3302 (NH).

Synthesis of [PhBP$^{Ph}_3$]Fe(OAc)(CO), 12. A suspension of Pb(OAc)$_4$ in 1 mL of THF (13.5 mg, 0.0305 mmol) was added dropwise to a stirring solution of **6** (24.4 mg, 0.0305 mmol) in 2 mL of THF. An immediate color change from orange to green was noted, and after stirring for an additional 12 h, the volatiles were removed to yield a green residue. The solids were rinsed with pentane, extracted into benzene, filtered, and lyophilized. The green powder was then taken up in THF and layered with pentane to yield crystalline material suitable for XRD (12.0 mg, 47.5%). ^{1}H NMR (C_6D_6, 300 MHz): δ 8.13 (d, J = 6.8 Hz, 2H), 7.77 (bs, 4 H), 7.69 (t, J = 7.3 Hz, 2H), 7.42 (bs, 6H), 7.31 (t, J = 8.4 Hz, 4H), 6.99 (bs, 6H), 6.90 (bs, 4H), 6.82 (bs, 4H), 6.73 (t, J = 7.0 Hz, 3H), 2.1−2.3 (m, 4H), 1.76 (bs, 2H), 1.47 (s, 3H). ^{31}P NMR (121 MHz, C_6D_6): δ 48.58 (d, J = 66.3 Hz, 2P), 29.81 (t, J = 66.4 Hz, 1P). IR (KBr) (cm^{-1}): 1976 (CO), 1469. Anal. Calcd. for $C_{48}H_{44}BFeO_2P_3$: C 69.59; H 5.35; N 0. Found: C 69.76; H 5.50; N 0.

Synthesis of {[PhBP$^{Ph}_3$]Fe(η^2-N_2H_4)(CO)}(PF$_6$), 13. A suspension of [Fc](PF$_6$) (15.0 mg, 0.0455 mmol) in 1 mL of benzene was added dropwise to a stirring solution of **6** (36.4 mg, 0.0455 mmol) in 2 mL of benzene. The reaction stirred for 24 h, during which a color change from orange to red ensued. The reaction mixture was lyophilized, and the resulting solids were rinsed with pentane and diethyl ether. The remaining solids were extracted into THF, filtered, and layered with pentane, yielding analytically pure crystals suitable for XRD (18.2 mg, 42.3%). ^{1}H NMR (C_6D_6, 300 MHz): δ 8.03 (bs, 2H), 7.66 (bs, 5H), 7.41 (bs, 5H), 7.03 (bs, 8H), 6.5−6.8 (m, 15H). ^{31}P NMR (C_6D_6, 300 MHz): δ 50.22 (d, $^1J_{PP}$ = 63.6 Hz, 2P), 36.00 (t, $^1J_{PP}$ = 63.6 Hz, 1P), −142.7 (m, 1P). IR (KBr) (cm^{-1}): 3332, 3276, 3253, 1986 (CO). Anal. Calcd. for $C_{46}H_{45}BFeN_2OP_4F_6$: C 58.35; H 4.79; N 2.96. Found: C 58.56; H 5.02; N 2.60.

■ ASSOCIATED CONTENT

Ⓢ Supporting Information

Detailed experimental procedures for reactions with quinones, NMR spectra of **2** and **5**, and crystal structure figures are

dx.doi.org/10.1021/ic301704f | Inorg. Chem. 2012, 51, 10043−10054

included in the Supporting Information (.pdf). Crystallographic details for all structures are provided in CIF format. This material is available free of charge via the Internet at http://pubs.acs.org.

AUTHOR INFORMATION

Corresponding Author

*E-mail: jpeters@caltech.edu.

Present Address

[†]Department of Chemistry, University of Minnesota, Minneapolis, Minnesota 55455.

Notes

The authors declare no competing financial interest.

ACKNOWLEDGMENTS

Dr. David VanderVelde, and Dr. Jeff Simpson are acknowledged for insightful discussions regarding the NMR spectroscopy of the compounds. Dr. Peter Müller, Dr. Michael Day, and Dr. Larry Henling are acknowledged for insightful discussions regarding X-ray crystallography. This work was generously supported by the NIH (GM-070757), and the Gordon and Betty Moore Foundation. Funding for the Caltech NMR facility was provided in part by the NIH (RR 027690). C.T.S. is grateful for an NSF graduate fellowship.

REFERENCES

(1) (a) Hoffman, B. M.; Dean, D. R.; Seefeldt, L. C. *Acc. Chem. Res.* **2009**, *42*, 609. (b) Howard, J. B.; Rees, D. C. *Proc. Natl. Acad. Sci. U.S.A.* **2006**, *103*, 17088. (c) Dance, I. *Dalton Trans.* **2010**, *39*, 2972. (d) Kästner, J.; Blöchl, P. E. *J. Am. Chem. Soc.* **2007**, *129*, 2998. (e) Hinnemann, B.; Nørskov, J. K. *J. Am. Chem. Soc.* **2004**, *126*, 3920. (f) Crossland, J. L.; Tyler, D. R. *Coord. Chem. Rev.* **2010**, *254*, 1883.

(2) (a) Barney, B. M.; Lukoyanov, D.; Igarashi, R. Y.; Laryukhin, M.; Yang, T. C.; Dean, D. R.; Hoffman, B. M.; Seefeldt, L. C. *Biochemistry* **2009**, *48*, 9094. (b) Barney, B. M.; Yang, T.-C.; Igarashi, R. Y.; Dos Santos, P. C.; Laryukhin, M.; Lee, H.-I.; Hoffman, B. M.; Dean, D. R.; Seefeldt, L. C. *J. Am. Chem. Soc.* **2005**, *127*, 14960. (c) Barney, B. M.; Laryukhin, M.; Igarashi, R. Y.; Lee, H.-I.; Dos Santos, P. C.; Yang, T.-C.; Hoffman, B. M.; Dean, D. R.; Seefeldt, L. C. *Biochemistry* **2005**, *44*, 8030.

(3) (a) Barney, B. M.; McClead, J.; Lukoyanov, D.; Laryukhin, M.; Yang, T. C.; Dean, D. R.; Hoffman, B. M.; Seefeldt, L. C. *Biochemistry* **2007**, *46*, 6784. (b) Barney, B. M.; Lukoyanov, D.; Yang, T. C.; Dean, D. R.; Hoffman, B. M.; Seefeldt, L. C. *Proc. Natl. Acad. Sci. U.S.A.* **2006**, *103*, 17113. (c) Danyal, K.; Inglet, B. S.; Vincent, K. A.; Barney, B. M.; Hoffman, B. M.; Armstrong, F. A.; Dean, D. R.; Seefeldt, L. C. *J. Am. Chem. Soc.* **2010**, *132*, 13197. (d) Lukoyanov, D.; Dikanov, S. A.; Yang, Z.-Y.; Barney, B. M.; Samoilova, R. I.; Narasimhulu, K. V.; Dean, D. R.; Seefeldt, L. C.; Hoffman, B. M. *J. Am. Chem. Soc.* **2011**, *133*, 11655.

(4) (a) Li, Y.; Shi, Y.; Odom, A. L. *J. Am. Chem. Soc.* **2004**, *126*, 1794. (b) Hoover, J. M.; DiPasquale, A.; Mayer, J. M.; Michael, F. E. *J. Am. Chem. Soc.* **2010**, *132*, 5043. (c) Herrmann, H.; Lloret Fillol, J.; Wadepohl, H.; Gade, L. H. *Angew. Chem., Int. Ed.* **2007**, *46*, 8426. (d) Huang, Z.; Zhou, J.; Hartwig, J. F. *J. Am. Chem. Soc.* **2010**, *132*, 11458.

(5) (a) Herrmann, H.; Wadepohl, H.; Gade, L. H. *Dalton Trans.* **2008**, 2111. (b) Cowie, M.; Gauthier, M. D. *Inorg. Chem.* **1980**, *19*, 3142. (c) Latham, I. A.; Leigh, G. J.; Huttner, G.; Jibril, I. *J. Chem. Soc., Dalton Trans.* **1986**, 385. (d) Carroll, J. A.; Sutton, D. *Inorg. Chem.* **1980**, *19*, 3137. (e) Dilworth, J. R.; Henderson, R. A.; Dahlstrom, P.; Nicholson, T.; Zubieta, J. A. *J. Chem. Soc., Dalton Trans.* **1987**, 529.

(6) (a) Chatt, J.; Pearman, A. J.; Richards, R. L. *J. Chem. Soc., Dalton Trans.* **1977**, 2139. (b) Takahashi, T.; Mizobe, Y.; Sato, M.; Uchida, Y.; Hidai, M. *J. Am. Chem. Soc.* **1979**, *101*, 3405. (c) Dilworth, J. R.; Lewis, J. S.; Miller, J. R.; Zheng, Y. *J. Chem. Soc., Dalton Trans.* **1995**, 1357. (d) Lee, Y. H.; Mankad, N. P.; Peters, J. C. *Nat. Chem.* **2010**, *2*, 558. (e) Schrock, R. R.; Liu, A. H.; O'Regan, M. B.; Finch, W. C.; Payack, J. F. *Inorg. Chem.* **1988**, *27*, 3574. (f) Schrock, R. R.; Glassman, T. E.; Vale, M. G.; Kol, M. *J. Am. Chem. Soc.* **1993**, *115*, 1760. (g) Cai, S.; Schrock, R. R. *Inorg. Chem.* **1991**, *30*, 4105. (h) Vale, M. G.; Schrock, R. R. *Organometallics* **1991**, *10*, 1661. (i) Vogel, S.; Barth, A.; Huttner, G.; Klein, T.; Zsolnai, L.; Kremer, R. *Angew. Chem., Int. Ed. Engl.* **1991**, *30*, 303. (j) Crossland, J. L.; Balesdent, C. G.; Tyler, D. R. *Dalton Trans.* **2009**, 4420. (k) McCleverty, J. A.; Rae, A. E.; Wolochowicz, I.; Bailey, N. A.; Smith, J. M. A. *J. Chem. Soc., Dalton Trans.* **1983**, 71. (l) McCleverty, J. A.; Rae, A. E.; Wolochowicz, I.; Bailey, N. A.; Smith, J. M. A. *J. Chem. Soc., Dalton Trans.* **1983**, 71. (m) Shapiro, P. J.; Henling, L. M.; Marsh, R. E.; Bercaw, J. E. *Inorg. Chem.* **1990**, *29*, 4560. (n) Field, L. D.; Li, H. L.; Dalgarno, S. J.; Jensen, P.; McIntosh, R. D. *Inorg. Chem.* **2011**, *50*, 5468.

(7) (a) Vale, M. G.; Schrock, R. R. *Inorg. Chem.* **1993**, *32*, 2767. (b) Shaver, M. P.; Fryzuk, M. D. *J. Am. Chem. Soc.* **2005**, *127*, 500. (c) Latham, I. A.; Leigh, G. J. *J. Chem. Soc., Dalton Trans.* **1986**, 399.

(8) Saouma, C. T.; Kinney, R. A.; Hoffman, B. M.; Peters, J. C. *Angew. Chem., Int. Ed.* **2011**, *50*, 3446.

(9) (a) Betley, T. A.; Peters, J. C. *J. Am. Chem. Soc.* **2004**, *126*, 6252. (b) Brown, S. D.; Betley, T. A.; Peters, J. C. *J. Am. Chem. Soc.* **2003**, *125*, 322. (c) Brown, S. D.; Mehn, M. P.; Peters, J. C. *J. Am. Chem. Soc.* **2005**, *127*, 13146. (d) Brown, S. D.; Peters, J. C. *J. Am. Chem. Soc.* **2005**, *127*, 1913. (e) Mankad, N. P.; Whited, M. T.; Peters, J. C. *Angew. Chem., Int. Ed.* **2007**, *46*, 5768. (f) Mehn, M. P.; Peters, J. C. *J. Inorg. Biochem.* **2006**, *100*, 634. (g) Betley, T. A.; Peters, J. C. *J. Am. Chem. Soc.* **2003**, *125*, 10782.

(10) Saouma, C. T.; Peters, J. C. *Coord. Chem. Rev.* **2011**, *255*, 920.

(11) Saouma, C. T.; Moore, C. E.; Rheingold, A. L.; Peters, J. C. *Inorg. Chem.* **2011**, *50*, 11285.

(12) Saouma, C. T.; Müller, P.; Peters, J. C. *J. Am. Chem. Soc.* **2009**, *131*, 10358.

(13) (a) Lu, C. C.; Saouma, C. T.; Day, M. W.; Peters, J. C. *J. Am. Chem. Soc.* **2007**, *129*, 4. (b) Betley, T. A.; Peters, J. C. *Inorg. Chem.* **2003**, *42*, 5074. (c) Peters, J. C.; Feldman, J. D.; Tilley, T. D. *J. Am. Chem. Soc.* **1999**, *121*, 9871. (d) Shapiro, I. R.; Jenkins, D. M.; Thomas, J. C.; Day, M. W.; Peters, J. C. *Chem. Commun.* **2001**, 2152.

(14) (a) Yandulov, D. V.; Schrock, R. R. *Science* **2003**, *301*, 76. (b) Ni, C.; Fettinger, J. C.; Long, G. J.; Brynda, M.; Power, P. P. *Chem. Commun.* **2008**, 6045. (c) Nguyen, T.; Sutton, A. D.; Brynda, M.; Fettinger, J. C.; Long, G. J.; Power, P. P. *Science* **2005**, *310*, 844.

(15) Lu, C. C. *The Chemistry of Tris(phosphino)borate Manganese and Iron Platforms*; Caltech: Pasadena, CA, 2006.

(16) Brown, S. D.; Peters, J. C. *J. Am. Chem. Soc.* **2004**, *126*, 4538.

(17) Mason, J. *Chem. Rev.* **1981**, *81*, 205.

(18) Field, L. D.; Li, H. L.; Dalgarno, S. J.; Turner, P. *Chem. Commun.* **2008**, 1680.

(19) Crossland, J. L.; Zakharov, L. N.; Tyler, D. R. *Inorg. Chem.* **2007**, *46*, 10476.

(20) Müller, P.; Herbst-Irmer, R.; Spek, A. L.; Schneider, T. R.; Sawaya, M. R. *Crystal Structure Refinement: A Crystallographer's Guide to SHELXL*; Oxford University Press: Oxford, U.K., 2006.

(21) Fox, D. J.; Bergman, R. G. *Organometallics* **2004**, *23*, 1656.

(22) Sellmann, D.; Hille, A.; Rösler, A.; Heinemann, F. W.; Moll, M.; Brehm, G.; Schneider, S.; Reiher, M.; Hess, B. A.; Bauer, W. *Chem.—Eur. J.* **2004**, *10*, 819.

(23) Foner, S. N.; Hudson, R. L. *J. Chem. Phys.* **1978**, *68*, 3162.

(24) Sellmann, D.; Soglowek, W.; Knoch, F.; Moll, M. *Angew. Chem., Int. Ed. Engl.* **1989**, *28*, 1271.

(25) (a) Sellmann, D.; Böhlen, E.; Waeber, M.; Huttner, G.; Zsolnai, L. *Angew. Chem., Int. Ed. Engl.* **1985**, *24*, 981. (b) Collman, J. P.; Hutchison, J. E.; Lopez, M. A.; Guilard, R.; Reed, R. A. *J. Am. Chem. Soc.* **1991**, *113*, 2794.

(26) Huttner, G.; Gartzke, W.; Allinger, K. *Angew. Chem., Int. Ed. Engl.* **1974**, *13*, 822.

(27) Sellmann, D. *J. Organomet. Chem.* **1972**, *44*, C46.

(28) Fujisawa, K.; Lehnert, N.; Ishikawa, Y.; Okamoto, K.-i. *Angew. Chem., Int. Ed.* **2004**, *43*, 4944.

(29) Smith, M. R.; Cheng, T. Y.; Hillhouse, G. L. *J. Am. Chem. Soc.* **1993**, *115*, 8638.
(30) (a) Cheng, T. Y.; Peters, J. C.; Hillhouse, G. L. *J. Am. Chem. Soc.* **1994**, *116*, 204. (b) Albertin, G.; Antoniutti, S.; Giorgi, M. T. *Eur. J. Inorg. Chem.* **2003**, *2003*, 2855.
(31) Cheng, T.-Y.; Ponce, A.; Hillhouse, G. L.; Rheingold, A. L. *Angew. Chem., Int. Ed. Engl.* **1994**, *33*, 657.
(32) Crossland, J. L.; Balesdent, C. G.; Tyler, D. R. *Inorg. Chem.* **2011**, *51*, 439.
(33) Moret, M.-E.; Peters, J. C. *J. Am. Chem. Soc.* **2011**, *133*, 18118.
(34) Warren, J. J.; Tronic, T. A.; Mayer, J. M. *Chem. Rev.* **2010**, *110*, 6961.
(35) Schubert, E. M. *J. Chem. Educ.* **1992**, *69*, 62.
(36) Sheldrick, G. M. *Acta Crystallogr.* **1990**, *A46*, 467.
(37) Sheldrick, G. M. *Acta Crystallogr.* **2008**, *A64*, 112.
(38) Du, C. J. F.; Hart, H.; Ng, K. K. D. *J. Org. Chem.* **1986**, *51*, 3162.
(39) Tang, H.; Richey, H. G. *Organometallics* **2001**, *20*, 1569.
(40) Armarego, W. L. F.; Chai, C. L. L. *Purification of Laboratory Chemicals*, 5th ed.; Butterworth-Heinmann: London, U.K., 2002.